

We thank the Co-Editor for the thorough revision and for providing constructive comments on our manuscript, **"Observed trends in ground-level O₃ in Monterrey, Mexico during 1993-2014: Comparison with Mexico City and Guadalajara"**. We are pleased that the Co-Editor editor's perspective on addressing O₃ long-term trends in Mexican urban areas is in agreement with our own views on the issue. We have addressed the concerns and recommendations received, and we believe that these helped to improve significantly the quality of our manuscript. Please find below our detailed response to the comments received, which are also highlighted in yellow in the revised version of the manuscript, submitted along with this response. Please note that sections 3 and 4 have few marks since there were included during the last revision as requested by the Co-Editor.

Co-Editor Decision: Reconsider after major revisions (19 Feb 2017) by Sally E. Pusede
Comments to the Author: Review Hernandez Paniagua et al.

I appreciate that the authors have responded to the comments of the referees, but I have some major concerns that need to be addressed prior to publication.

1. My primary issue is the paper lacks focus and, after reading, I am not sure what the authors were trying to communicate scientifically about O_x trends in the urban areas in Mexico studied. Instead, the paper is largely descriptive, presenting many trends, but without clear purpose. It is insufficient for publication in ACP to describe a wide array of measurements and then speculate on the causes of the observed patterns. While there are few studies on O_x in Mexico, too much is known about urban O_x chemistry generally for pages of text to describe O_x seasonal trends and diurnal patterns. If the O_x AVd metric is being interpreted as a proxy for O₃ production, then say this explicitly. Trends in O₃ AVd may simply indicate changes in NO₂.

Response: We highlight that our primary aim is to address the effect of the few controls introduced to control precursor emissions on ground-level O₃ long-term trends and on the air quality within the MMA. Second, we also investigate if the strategies designed to control O₃ precursor emissions within the MCMA, which have been introduced at the GMA and at the MMA have resulted in improvements in terms of decreasing the O₃ levels. We have clarified that very different air quality control strategies have been considered at each city studied here, which has led to different air pollution scenarios at each one. For example, while the Mexico City has been subject of numerous measures focused on emissions from on-road, point and area emissions, the measures implemented at Monterrey has been focused mostly on on-road sources with less consideration to other emissions sources, which has occurred also at the GMA. Furthermore, although on-road sources are reported to contribute with more than 50 % of total primary emissions at Monterrey, the location of the largest industrial area upwind the urban core has caused that growing industrial emissions offset the reductions in emissions from on road sources.

To estimate the absolute changes in net O₃ production, first, we describe how primary emissions impact the net O₃ production at each monitoring site at different time-scales. We use daily and annual cycles to interpret how the levels of O₃ and O_x vary with the levels of NO_x, and interpret the long-term trends as the response to changes in precursor emissions. We also compared the trends for O₃ precursors derived from available ground-based measurements at each city, with those determined from emission estimates, showing that significant improvements in such estimates are required to better inform the current air quality policies. Finally, we revised the number of O₃ annual exceedances to the O₃ official standards, and show that if primary emissions maintain the current trends, the number of annual exceedances to the official standards will very likely increase.

2. Second, the Introduction states that the authors are concerned with O_x trends based on health-based metrics (page 4, line 135). It is not obvious to me then that a discussion of wintertime (and possibly springtime) trends is even warranted.

Response: This statement was requested by a referee during the last revision, however, after the major changes have been made it has been deleted. We have clarified that our main objective is the assessment of trends in O_3 and O_x in response to changes in precursor emissions. The compliance of the Mexican standards for O_3 is carried out to show that if O_3 levels continue increasing more exceedances will occur.

3. Additionally, annual average assessments obscure summertime differences, which, if concerned with high O_3 (health-based metrics), should be the focus. To this aim, I see the presentation of trends in annual average O_x and AVd to be a distraction, as they may track wintertime changes (generally always VOC-limited chemistry), rather than changes in summertime O_3 production (potentially VOC or NOx limited). Consideration of the 95th percentile O_3 trends is likely a de facto summertime trend, but this is never stated nor are the data analyzed in this context.

Response: We have separated the analysis of O_3 long-term trends, considering now seasonal trends as reported by Parrish et al. (2009), and discussed the results accordingly. Briefly, we show that the significant trends observed are consistent with the transport of emissions from the industrial area, enhanced during spring and summer.

4. I recommend the authors provide the reader with a focused statement of purpose and then only present observations relevant to this task.

Response: As requested, the objectives description paragraph of our study were modified accordingly. Additionally, a paragraph describing the paper organisation was also included. Text modified: " To our knowledge, no previous study has address trends in O_3 and odd oxygen in urban areas of Mexico. In this study, we describe trends in ground-level O_3 within the MMA, and its response to changes in precursor emissions during 1993-2014. Long-term and high-frequency measurements of O_3 were recorded at 5 air quality monitoring stations evenly distributed within the MMA. In order to better assess photo-chemical production of O_3 , odd oxygen defined as ($[O_x] = [O_3] + [NO_2]$) was also considered, as O_3 and NO_2 are rapidly interconverted. Diurnal and annual cycles of O_3 and O_x are used to interpret net O_3 production within the MMA. We show that air mass origin influences strongly the O_3 annual growth rates. The trends in O_3 , O_x and precursor emissions are compared with those observed within the MCMA and GMA. Finally, we describe that NEI emission estimates for NO_x and VOCs disagree in the trend magnitudes with ground-based NO_x and VOCs measurements made at the urban areas studied here.

This paper is organised as follows: Section 2 presents the data quality and methodology used to derived the different trends presented. Section 3 describes in detail the O_3 and O_x diurnal and annual cycles, and, annual and seasonally averaged trends. Section 4 discusses the origin of the O_3 and O_x diurnal variations and trends in the light of changes in precursor emissions. Finally, Section 5 provides some conclusions regarding the trends observed at the studied urban areas.".

5. For me, an inter-annual high-O_x trend analysis would be an incredibly valuable contribution to the literature.

Response: As requested, we have also included the analysis of seasonal high O₃ trends. Briefly, we show that if O₃ precursor emissions continue increasing the daily maxima will likely increase and that the number of annual exceedances to the O₃ official standard will also increase.

6. I also recommend the authors present separate Results and Discussion sections. This would ensure the paper escapes the trap of presenting an observation and then immediately speculating on the cause. For example, this is done three times in the paragraph on page 9, lines 321–330, but is ubiquitous throughout the manuscript.

Response: As requested, we now present results and discussion in separate sections. See sections 3 and 4.

Minor comments:

Abstract, line 15. "In developed countries, long-term trends in O₃ have been studied extensively." I would not say this is true.

Response: We rephrased the sentence to clarify that high O₃ levels have been an historic problem at large Mexican urban areas. Text modified: "The largest urban areas in Mexico have experienced historically high ambient O₃ levels." See line: 17.

Page 2, line 45. "being VOC-limited" should say "being called VOC-limited."

Response: The statement was modified. Text modified: " The system of O₃ production is not linear, and is termed NO_x-limited, when O₃ production increases in response to increasing NO_x emissions, and termed VOC-limited when it responds positively to emissions of VOCs (Monks et al., 2015; Pusede et al., 2015).". See lines: 45-47.

Page 2, line 55. The reaction between NO and O₃ is not an O₃ loss process, as NO₂ immediately photolyzes to yield O₃. At night NO₂ simply stores O₃.

Response: As requested, the sentence was modified. Text modified: " By contrast, the main removal processes for tropospheric O₃ are photochemical loss and dry deposition (Atkinson, 2000; Jenkin and Clemitshaw, 2000).". See lines: 55-56.

Page 2, line 64–75. Discussion of trends in background and annual O₃ is irrelevant to this analysis. Remove from Introduction.

Response: The lines describing trends in annual background O₃ were removed as requested.

Page 3, lines 81–82. Are you quoting trends in emission inventories or in actual trends? Make this clear. Should also say that there is variability between cities.

Response: We clarified that the decrease in NO_x and VOCs emissions quoted was derived from emissions estimates, and also that this decline was estimated at national scale despite the variability from city-to-city. Text modified: "Emission estimates suggest an overall national scale decrease during 1980-2008 in US NO_x and VOCs emissions of 40 % and 47 %, respectively, with city-to-city variability (EPA, 2009; Xing et al., 2013). " See lines: 75-76.

Page 3, line 96. A decrease of 33% in what?

Response: We clarified that the 33 % decrease described corresponds to that in O₃ annual averages. Text modified: "...with reports of a decrease in O₃ annual averages of ca. 33 % during the last two decades" See lines: 90-91.

Page 3, line 96. Delete "By contrast."

Response: As requested, "By contrast," was deleted. Text modified: "O₃ has received less consideration at other large metropolitan areas, where Mexican air quality standards are frequently exceeded (Table 1)." See lines: 91-93.

Page 3, line 97. Delete "relatively."

Response: As requested, "relatively" was deleted. See previous comment. See line: 92.

Page 3, lines 100–101. Not clear what this means: "has breached the 1-h average standard of 110 ppb O₃ by up to 80 %."

Response: The sentence was rephrased to clarify that the O₃ mixing ratios recorded at the GMA and at the MMA have exceeded the O₃ official standards by more than 50 %. Text modified: "Indeed, since 2000, recorded O₃ mixing ratios have exceeded Mexican official standards for O₃ 1-h average (110 ppb) and 8-h running average (80 ppb) by more than 50 % at the Guadalajara metropolitan area (GMA, the second most populated city) and at the Monterrey metropolitan area (MMA, the third most populated city (INE, 2011; SEMARNAT, 2015)." See lines: 93-96.

Page 3, lines 104–106. Critical without point. Remove or rephrase.

Response: The sentence was rephrased to clarify that the ordinary linear regression used by Benítez-García et al. (2014) is not suitable for determining long-term trends, because this can be biased by the presence of extreme data. Text modified: "However, it should be noted that the ordinary linear regression analysis used by Benítez-García et al. (2014) may be biased by extreme values and is therefore not suitable to determine O₃ long-term trends with significant confidence." See lines: 98-101.

Page 3, line 109. What is meant by "data?"

Response: The sentence was rephrased to clarify that the implemented initiatives have been designed on the basis of emission estimates reported in the NEI. Text modified: "The NEI suggest that from 1999 to 2008, anthropogenic NO_x emissions decreased at the MCMA by 3.8 % yr⁻¹, but increased at the GMA and the MMA by 1.9 % yr⁻¹, and by 4.0 % yr⁻¹, respectively (Fig. S1) (SEMARNAT, 2006, 2011, 2014)." See lines: 105-107.

Page 4, lines 137–140. This statement is problematic: "The data sets contain features representative of industrial, urban-background and urban monitoring sites, which allow assessment of O₃ trends and dynamics, pollutant emissions and their contribution to the atmospheric composition depending on local meteorology and air mass transport." Really the data allow you to - assess ozone trends in locations with mixed sources and variable meteorology.

Response: We modified the objectives paragraph and removed the sentence regarding the dataset description. Text modified: "To our knowledge, no previous study has address trends in O₃ and odd oxygen in urban areas of Mexico. In this study, we describe trends in ground-level O₃ within the MMA, and its response to changes in precursor emissions during 1993-2014. Long-term and high-frequency measurements of O₃ were recorded at 5

air quality monitoring stations evenly distributed within the MMA. In order to better assess photo-chemical production of O_3 , odd oxygen defined as ($[O_x] = [O_3] + [NO_2]$) was also considered, as O_3 and NO_2 are rapidly interconverted. Diurnal and annual cycles of O_3 and O_x are used to interpret net O_3 production within the MMA. We show that air mass origin influences strongly the O_3 annual growth rates. The trends in O_3 , O_x and precursor emissions are compared with those observed within the MCMA and GMA. Finally, we describe that NEI emission estimates for NO_x and VOCs disagree in the trend magnitudes with ground-based NO_x and VOCs measurements made at the urban areas studied here" See lines: 130-139.

Page 4, lines 141–142. Change “oxidants” to “odd oxygen.” A clearer way to say - O_x include O_3 stored as NO_2 .
Response: As requested: total oxidants as replaced with "odd oxygen". See line: 134.

Page 4, lines 142–143. Sentence is not meaningful.

Response: We modified the paragraph describing the aims of this study to make clear that O_3 diurnal and annual cycles are interpreted as proxy of net O_3 production. Text modified: "Diurnal and annual cycles of O_3 and O_x are used to interpret net O_3 production within the MMA." See lines: 135-136.

Page 6, line 207. This subtitle should not be “Analysis of data,” which implies scientific consideration of the data.

Response: The subtitle was changed to "Analytical methods". See line: 207.

Page 9, lines 307–309. Irrelevant, delete: “A study conducted among asthmatic children resident in the MCMA revealed an increase in coughing and wheezing rates, associated with cumulative exposure to high 1-h averages mixing ratios of O_3 and NO (Escamilla-Nuñez et al., 2008).”

Response: As requested, the sentence was deleted and the whole section split into Results and Discussion sections.

Page 9, 313–314. Speculation at best, “likely influenced by the significant ($p<0.05$) annual growth of 1.90 ppb y-1 in NO in levels as shown in Fig. 4.” Best to have a separate Results and Discussion section.

Response: As requested, Results and Discussion are presented in separate sections. See sections 3 and 4.

Page 9, 322–323. Speculation - “which arise either from an increment in NO_x or O_3 levels as shown in Fig. 4.” Either give evidence for this statement or delete.

Response: We provide evidence to confirm that the increment in daily maximum 1-h O_3 arises from increases in NO_x . See lines: 483-493.

Page 9, 324–325. Speculative: - “ O_x trend is likely due to the decreasing levels of NO_x .” Give evidence or delete.

Response: We provide evidence to confirm that at OBI, O_x has decreased in response to decreases in NO_x emissions from the on-road sources, which only can be appreciated at OBI, since at the rest of the sites, NO_x industrial emissions offset those reductions. See lines: See section 3.6 and 4.4.

Page 9, 328–330. Speculation - “This could be due to the arrival at OBI and at STA of chemically processed air masses with decreased VOC/ NO_x ratios, compared with those arriving at SNN loaded with fresh emissions from the nearby industrial area.”

Response: See the previous comment. See section 4.4 and Fig. S10.

Page 14, line 519. Need to verify there is also no weekend effect in O_x .

Response: The existence of weekend effect in O_x was tested for all urban areas, and shown in Fig. 8. We describe that no significant differences were observed both in O_3 and O_x in each city. See lines: 395-411.

1 **Observed trends in ground-level O₃ in Monterrey, Mexico during 1993-2014: Comparison with**
2 **Mexico City and Guadalajara**

4 Iván Y. Hernández Paniagua^{1,2}, Kevin C. Clemitsaw³, and Alberto Mendoza^{1,*}

6 ¹Escuela de Ingeniería y Ciencias, Tecnológico de Monterrey, Campus Monterrey, Av.
7 Eugenio Garza Sada 2501, Monterrey, N.L., México, 64849.

8 ²Centro de Ciencias de la Atmosfera, Universidad Nacional Autónoma de México, Circuito Exterior de
9 Ciudad Universitaria, Ciudad de México, 04510, México

10 ³Department of Earth Sciences, Royal Holloway University of London, Egham, Surrey TW20 0EX, UK.

11 *Corresponding author: mendoza.alberto@itesm.mx

13 **Keywords**

14 Air quality, emissions inventory, odd oxygen, time series, wind-sector analysis

16 **Abstract**

17 The largest urban areas in Mexico have experienced historically high ambient O₃ levels. Here, we
18 present an assessment of long-term trends in O₃ and odd oxygen (O₃ + NO₂) at the industrial Monterrey
19 metropolitan area (MMA) in NE Mexico. High-precision and high-frequency UV-photometric
20 measurements of ambient O₃ have been made since 1993 at 5 sites within the MMA. Diurnal amplitudes
21 in O₃ (AV_d) are used as a proxy for net O₃ production, which is influenced by the NO₂ photolysis rate. No
22 significant differences are observed in the AV_d during weekdays when fossil fuel use and combustion
23 process are higher than during weekends, although the largest AV_d are observed at sites downwind of
24 industrial areas. During weekdays, cycle troughs and peaks are typically recorded at 07:00 and 14:00
25 CDT, respectively, and during weekends, at 06:00 and 13:00 CDT, respectively.

26
27 The O₃ annual cycle is driven by changes in meteorology and photochemistry, with maximum O₃ mixing
28 ratios recorded in spring and minimum values in winter. The largest annual variations in O₃ are typically
29 observed downwind of the MMA, with the lowest variations generally recorded in highly populated areas
30 and close to industrial areas. A wind sector analysis shows that, at all sites, the highest O₃ mixing ratios
31 are typically recorded from the E and SE sectors, while the lowest values are recorded in air masses
32 from the W and NW. A wind sector analysis of mixing ratios of O₃ precursors revealed that the dominant
33 sources of emissions are located in the industrial regions within the MMA and the surrounding area.
34 Significant increasing trends in O₃ in spring, summer and autumn are observed depending on site
35 location, with trends in annual averages ranging between 0.19 and 0.33 ppb yr⁻¹. The largest annual
36 increases in O₃ are for the E and SE sectors, 0.50 and 0.66 ppb yr⁻¹, respectively. Overall, during 1993
37 to 2014, within the MMA, O₃ has increased at an average rate of 0.22 ppb yr⁻¹ ($p<0.01$), which is in
38 marked contrast with the decline of 1.15 ppb yr⁻¹ ($p<0.001$) observed in the Mexico City metropolitan

39 area (MCMA) for the same period. No clear trend is observed during 1996 to 2014 within the Guadalajara
40 metropolitan area (GMA).

41

42 1. Introduction

43 O₃ is a secondary air pollutant formed in the troposphere via the photo-oxidation of CO, methane (CH₄)
44 and volatile organic compounds (VOCs) in the presence of NO and NO₂ (NO + NO₂ = NO_x) (Jenkin and
45 Clemitshaw, 2000). The system of O₃ production is not linear, and is termed NO_x-limited, when O₃
46 production increases in response to increasing NO_x emissions, and termed VOC-limited when it
47 responds positively to emissions of VOCs (Monks et al., 2015; Pusede et al., 2015). Tropospheric O₃ is
48 of concern to policy makers due to its adverse impacts on human health, agricultural crops and
49 vegetation, and also due to its role as a greenhouse gas despite its relatively short lifetime of around
50 22.3 ± 3.0 days (Stevenson et al., 2006; IPCC, 2013; WHO, 2014; Lelieveld et al., 2015). As the
51 predominant source of OH, tropospheric O₃ controls the lifetime of CH₄, CO, VOCs, among many other
52 air pollutants (Revell et al., 2015). In polluted regions, increased levels of O₃ are prevalent during
53 seasons with stable high-pressure systems and intense photochemical processing of NO_x and VOCs
54 (Dentener et al., 2005; Xu et al., 2008) with downward transport from the stratosphere of lesser
55 importance (Wang et al., 2012). By contrast, the main removal processes for tropospheric O₃ are
56 photochemical loss and dry deposition (Atkinson, 2000; Jenkin and Clemitshaw, 2000).

57

58 Tropospheric O₃ increased in the Northern Hemisphere (NH) during 1950-1980s due to rapid increases
59 in precursor emissions during the industrialisation and economic growth of Europe and North America
60 (NA) (Staehelin and Schmid, 1991; Guicherit and Roemer, 2000). Since the 1990s, reductions in O₃
61 precursor emissions in economically developed countries have resulted in decreases in tropospheric O₃
62 levels (Schultz and Rast, 2007; Butler et al., 2012; Pusede et al., 2012), however, in some regions,
63 increases in O₃ have also been reported. For instance, from an analysis of O₃ data from 179 urban sites
64 over France during 1999-2012, Sicard et al. (2016) reported an increasing trend in the annual averages
65 of 0.14 ± 0.19 ppb yr⁻¹, and in the medians of 0.13 ± 0.22 ppb yr⁻¹, attributed to long-range transport and
66 reduced O₃ titration by NO due to reductions in local NO_x emissions. However, Sicard et al. (2016) also
67 reported during the same period that at 61 rural sites, O₃ decreased in the annual averages by 0.12 ±
68 0.21 ppb yr⁻¹, and in the medians by 0.09 ± 0.22 ppb yr⁻¹.

69

70 In the US and Canada, O₃ levels have decreased substantially at different metrics during the last two
71 decades in response to more stringent emission controls focused on on-road and industrial sources. In
72 the Greater Area of Toronto from 2000 to 2012, O₃ levels decreased at urban sites by approximately 0.4
73 % yr⁻¹, and at sub-urban sites by approximately 1.1 % yr⁻¹, as a consequence of a reduction in the mid-
74 day averages of NO₂ of 5.8 - 6.4 % yr⁻¹, and in the VOC reactivity of 9.3% yr⁻¹ (Pugliese et al., 2014).
75 Emission estimates suggest an overall national scale decrease during 1980-2008 in US NO_x and VOCs
76 emissions of 40 % and 47 %, respectively, with city-to-city variability (EPA, 2009; Xing et al., 2013).

77 Lefohn et al. (2010) reported that for 12 US major metropolitan areas, the O₃ US EPA exposure metrics
78 of the annual 2nd highest 1-h average, and the annual 4th highest daily maximum 8-h average, decreased
79 during 1980-2008 at 87 % and 71 % of the monitoring sites evaluated, respectively. However, Lefohn et
80 al. (2010) observed an increase in the lower- and mid-O₃ mixing ratios in response to decreased titration
81 by NO. More recently, Simon et al. (2015) assessed changes in the 1-h average O₃ mixing ratios at
82 around 1400 sites across the US between 1998-2013, using the 5th, 25th, 50th 75th 95th percentiles, and
83 the maximum daily 8-h average. Overall, Simon et al. (2015) observed increases at the lower end of the
84 O₃ data distribution of 0.1-1 ppb yr⁻¹, mostly in urban and sub-urban areas, whereas O₃ decreased at the
85 upper end of the data distribution between 1-2 ppb yr⁻¹ at less urbanised areas. Such changes were
86 associated with the implementation of control strategies within the US to abate peak O₃ mixing ratios, as
87 the NO_x SIP Call and, tighter point and vehicle emission standards.

88
89 In Mexico, studies of long-term trends in O₃ have focused on the Mexico City Metropolitan Area (MCMA)
90 (Molina and Molina, 2004; Jaimes et al., 2012; Rodriguez et al., 2016), with reports of a decrease in O₃
91 annual averages of ca. 33 % during the last two decades (Parrish et al., 2011; SEDEMA, 2016a). O₃ has
92 received less consideration at other large metropolitan areas, where Mexican air quality standards are
93 frequently exceeded (Table 1). Indeed, since 2000, recorded O₃ mixing ratios have exceeded Mexican
94 official standards for O₃ 1-h average (110 ppb) and 8-h running average (80 ppb) by more than 50 % at
95 the Guadalajara metropolitan area (GMA, the second most populated city) and at the Monterrey
96 metropolitan area (MMA, the third most populated city (INE, 2011; SEMARNAT, 2015). To date, only
97 Benítez-García et al. (2014) have addressed changes in ambient O₃ at the GMA and MMA during 2000-
98 2011, reporting an increase in O₃ annual averages of around 47 % and 42 %, respectively. However, it
99 should be noted that the ordinary linear regression analysis used by Benítez-García et al. (2014) may
100 be biased by extreme values and is therefore not suitable to determine O₃ long-term trends with
101 significant confidence.

102
103 To improve air quality, the Mexican government has introduced several initiatives to reduce primary
104 pollutants emissions, with emission estimates reported in the Mexican National Emissions Inventories
105 (NEI). The NEI suggest that from 1999 to 2008, anthropogenic NO_x emissions decreased at the MCMA
106 by 3.8 % yr⁻¹, but increased at the GMA and the MMA by 1.9 % yr⁻¹, and by 4.0 % yr⁻¹, respectively (Fig.
107 S1) (SEMARNAT, 2006, 2011, 2014). These NEI NO_x emission estimates agree with the decrease for
108 the MCMA of 1.7 % yr⁻¹ in the NO₂ vertical column density during 2005-2014 reported by Duncan et al.
109 (2016), but disagree for the GMA and the MMA where decreases of 2.7 % yr⁻¹ and of 0.3 % yr⁻¹,
110 respectively, are reported. Similarly, Boersma et al. (2008) observed that NO_x emissions over Mexico
111 derived from NO₂ satellite observations were higher by a factor of 1.5 - 2.5 times than bottom-up emission
112 estimates, which were lower by 1.6 - 1.8 times than data reported in the NEI 1999-base year. The NEI
113 anthropogenic VOCs emissions estimates suggest a decrease at the MMA by 0.2 % yr⁻¹, but increases
114 at the MCMA and at the GMA by 2.7 % yr⁻¹ and by 3.2 % yr⁻¹, respectively (Fig. S1) (SEMARNAT, 2006,

115 2011, 2014). However, as for NO_x, NEI trends in VOCs disagree with existing reports for average VOCs
116 decreases within the MCMA (Arriaga-colina et al., 2004; Garzón et al., 2015).

117
118 Local authorities have developed local emission inventories for the MCMA and the MMA, although only
119 for the MCMA the inventories have been compiled with a frequency of two years since 1996 (SEDEMA,
120 1999, 2001, 2003, 2004, 2006, 2008, 2010, 2012, 2014, 2016b; SDS, 2015). The accuracy of the MCMA
121 emission inventories has been also assessed during several field campaigns. For instance, during the
122 MCMA 2002-2003 campaign, Velasco et al. (2007) observed an overestimation in the 1998 inventory for
123 VOCs emissions of alkenes and aromatics, but an underestimation in the contribution of some alkanes.
124 By contrast, for the 2002 MCMA inventory, Lei et al. (2007) reported an underestimation in the VOCs
125 total emissions of around 65 %, based on a simulation of an O₃ episode occurred in 2003 within the
126 MCMA. Therefore, since these emission estimates are used to predict future air quality, and to design
127 clean air policies, it is imperative to examine the results of the policies implemented to control emissions
128 of O₃ precursors.

129
130 To our knowledge, no previous study has address trends in O₃ and odd oxygen in urban areas of Mexico.
131 In this study, we describe trends in ground-level O₃ within the MMA, and its response to changes in
132 precursor emissions during 1993-2014. Long-term and high-frequency measurements of O₃ were
133 recorded at 5 air quality monitoring stations evenly distributed within the MMA. In order to better assess
134 photo-chemical production of O₃, odd oxygen defined as ([O_x] = [O₃] + [NO₂]) was also considered, as
135 O₃ and NO₂ are rapidly interconverted. Diurnal and annual cycles of O₃ and O_x are used to interpret net
136 O₃ production within the MMA. We show that air mass origin influences strongly the O₃ annual growth
137 rates. The trends in O₃, O_x and precursor emissions are compared with those observed within the MCMA
138 and GMA. Finally, we describe that NEI emission estimates for NO_x and VOCs disagree in the trend
139 magnitudes with ground-based NO_x and VOCs measurements made at the urban areas studied here.

140
141 This paper is organised as follows: Section 2 presents the data quality and methodology used to derived
142 the different trends presented. Section 3 describes in detail the O₃ and O_x diurnal and annual cycles,
143 and, annual and seasonally averaged trends. Section 4 discusses the origin of the O₃ and O_x diurnal
144 variations and trends in the light of changes in precursor emissions. Finally, Section 5 provides some
145 conclusions regarding the trends observed at the studied urban areas.

146
147 **2. Methodology**

148 **2.1 Monitoring of O₃ in the Monterrey Metropolitan Area (MMA).**

149 The MMA (25°40'N, 100°20'W) is located around 720 km N of Mexico City, some 230 km S of the US
150 border in the State of Nuevo Leon (Fig. 1a). It lies at an average altitude of 500 m above sea level (m
151 asl) and is surrounded by mountains to the S and W, with flat terrain to the NE (Fig. 1b). The MMA is the
152 largest urban area in Northern Mexico at around 4,030 km², and is the third most populous in the country

153 with 4.16 million inhabitants, which in 2010, comprised 88 % of the population of Nuevo Leon State
154 (INEGI, 2010). It is the second most important industrial area in Mexico and has the highest gross
155 domestic product per capita (Fig. 1c). Although the weather changes rapidly on a daily time-scale, the
156 climate is semi-arid with an annual average rainfall of 590 mm, and an annual average temperature of
157 25.0°C with hot summers and mild winters (ProAire-AMM, 2008; SMN, 2016).

158

159 Within the MMA, tropospheric O₃, 6 additional air pollutants (CO, NO, NO₂, SO₂, PM₁₀, and PM_{2.5}) and 7
160 meteorological parameters (wind speed (WS), wind direction (WD), temperature (Temp), rainfall, solar
161 radiation (SR), relative humidity (RH) and pressure) have been monitored continuously, with data
162 summarised as hourly averages, since November 1992 at 5 stations that form part of the Integral
163 Environmental Monitoring System (SIMA) of the Nuevo Leon State Government (Table 2; SDS, 2016).
164 From November 1992 to April 2003, and in accordance with EPA, EQOA-0880-047, Thermo
165 Environmental Inc. (TEI) model 49 UV photometric analysers were used to measure O₃ with stated
166 precision less than ± 2 ppb O₃ and a detection limit of 2 ppb O₃. Similarly, in accordance with RFNA-1289-
167 074, TEI model 42 NO-O₃ chemiluminescence detectors were used to measure NO-NO₂-NO_x with stated
168 precision less than ± 0.5 ppb NO, and a detection limit of 0.5 ppb NO. In May 2003, replacement TEI
169 model 49C O₃ and model 42C NO-NO₂-NO_x analysers were operated as above, with stated precision
170 better than ± 1 ppb O₃ and ± 0.4 ppb NO, respectively, and detection limits of 1 ppb O₃ and 0.4 ppb NO,
171 respectively. To rule out instrumentation influences on the determined air pollutants trends, long-term
172 trends based on annual averages were compared with those derived using 3-yr running averages, in
173 accordance with Parrish et al. (2011) and Akimoto et al. (2015) (Supplementary Information S1.1; Fig.
174 S2). Calibration, maintenance procedures and quality assurance/quality control (QA/QC) followed
175 protocols established in the Mexican standards NOM-036-SEMARNAT-1993 and NOM-156-
176 SEMARNAT-2012. The SIMA dataset has been validated by the Research Division of Air Quality of the
177 Secretariat of Environment and Natural Resources (SEMARNAT). The monitoring of O₃ and other air
178 pollutants at the MCMA and the GMA is detailed in the Supplementary Information S1.2-3.

179

180 2.2 NEI data

181 NEI data for estimated NO_x and VOCs emissions for the 1999-, 2005- and 2008-base years were
182 obtained from the SEMARNAT website (<http://sinea.semarnat.gob.mx>). The data comprised emission
183 sources (mobile, point, area and natural) and air pollutants (NO_x, VOCs, SO_x, CO, PM_{2.5} and PM₁₀), at
184 national, state and municipality scales. The NEI emission estimates are developed in accordance with
185 the Manual for the Emission Inventories Program of Mexico (Radian, 2000), which is based on the US
186 EPA AP-42 emission factors categorisation (EPA, 1995). The emission factors are regionalised for each
187 Mexican state, based upon on-site measurements and survey information. Updates to the emission
188 factors have been conducted for each released NEI, although no changes in the methodology were
189 implemented between the 1999- and 2008-base years. Overall, the mobile emissions were estimated
190 using the MOBILE6-Mexico model (EPA, 2003). The emissions from point sources were derived using

191 the annual operation reports submitted to the Environment Ministry. The emissions from area sources
192 were obtained using the categorisation of Mexican area sources and the regionalised AP-42 emission
193 factors.

194

195 The MCMA emissions inventories have been developed with a 2-year frequency since 1996, and were
196 obtained from the MCMA Environment Secretariat website (<http://www.aire.cdmx.gob.mx/>). The
197 methodology used to construct the MCMA inventories estimates is consistent with that used in the NEI
198 (SEDEMA, 2016a), which is based on the AP-42 EPA emission factors. However, more speciated
199 emission factors have been developed in each released version, considering updates in the local
200 industrial activity, survey information and field measurement campaigns. To date, the only significant
201 change in the methodology is the replacement of the Mobile6-Mexico model with the MOVES model to
202 obtain the 2014-base year mobile emissions (SEDEMA, 2016b). As for the MCMA inventories, more
203 speciated emission factors than those contained in the NEI were developed to produce the MMA
204 emissions inventory 2013-base year (SDS, 2015), although, mobile emissions estimates were obtained
205 with the Mobile6-Mexico model (EPA, 2003).

206

207 **2.3 Analytical methods**

208 SIMA, SIMAT (Atmospheric Monitoring System of the MCMA) and SIMAJ (Atmospheric Monitoring
209 System of the GMA) instrumentation recorded O₃ data every minute, which were then validated and
210 archived as 1-h averages. Total SIMA O₃ data capture by year and site are shown in Fig. S3. Data
211 capture averaged during 1993-2014 ranged from 82.6 % at GPE to 93.3 % at SNB, with data capture
212 <50 % during 1998-2000 at GPE, in 1998 at SNN, and in 1999 at OBI. A threshold of 75% data capture
213 was defined to consider data valid and representative (ProAire-MMA, 2008; Zellweger et al., 2009;
214 Wilson et al., 2012). All data were processed with hourly averages used to determine daily averages,
215 which were used to calculate monthly averages, from which yearly averages were obtained.

216

217 **2.4 Data analysis methods**

218 The SIMA, SIMAT and SIMAJ O₃ data sets were analysed extensively using the *openair* package v. 1.1-
219 4 (Carslaw and Ropkins, 2012) for R software v. 3.1.2 (R Core Team, 2013). In this study, the *openair*
220 functions *windRose*, *timeVariation* and *TheilSen* were used to analyse air pollution data. Briefly, the
221 *windRose* summarises wind speed and wind direction by a given time-scale, with proportional paddles
222 representing the percentage of wind occurrence from a certain angle and speed range. The *timeVariation*
223 function was used to obtain normalised daily cycles by season, and weekly cycles, with the 95 %
224 confidence intervals in the cycles calculated from bootstrap re-sampling, which accounts for better
225 estimations for non-normally distributed data (Carslaw, 2015). Finally, long-term trends of air pollutants
226 at the MCMA, GMA and MMA were computed with the *TheilSen* function, which is based on the non-
227 parametric Theil-Sen method (Carslaw, 2015; and references therein). The Theil-Sen estimate of the
228 slope is the median of all slopes calculated for a given *n* number of x,y pairs, while the regression

229 parameters, confidence intervals and statistical significance are determined through bootstrap re-
230 sampling. It yields accurate confidence intervals despite the data distribution and heteroscedasticity, and
231 is also resistant to outliers.

232
233 The trends computed with *openair* were contrasted with those calculated using the MAKESENS 1.0
234 macro (Salmi et al., 2002) as follows. Firstly, the presence of a monotonic trend was tested with the non-
235 parametric Mann-Kendal test. For the MCMA, GMA and MMA, the available yearly data are $n > 10$, hence
236 positive values in the Z parameter correspond to positive trends and vice-versa for negative values of Z .
237 The significance of the estimated trend was tested at $\alpha = 0.001, 0.01, 0.05$ and 0.1 using a two-tailed test.
238 Secondly, slopes of linear trends were calculated with the non-parametric Sen's method, which assumes
239 linear trends, with a Q slope and a B intercept. To calculate Q , first the slopes of all data values were
240 calculated in pairs, with the Sen's estimator slope as the median of all calculated slopes. Finally, $100(1 -$
241 $\alpha)$ % two-sided confidence intervals about the slope estimate were obtained based on a normal
242 distribution. Comparisons of estimated trends from both approaches are shown in the Supplementary
243 information S1.4 (Fig. S4).

244
245 The O_3 and other air pollutant time-series were decomposed into trend, seasonal and residual
246 components using the Seasonal-Trend Decomposition technique (STL; Cleveland et al., 1990). STL
247 consists of two recursive procedures: an inner loop nested inside an outer loop, assuming measurements
248 of x_i (independent) and y_i (dependent) for $i = 1$ to n . The seasonal and trend components are updated
249 once in each pass through the inner loop; each complete run of the inner loop consists of $n_{(i)}$ such passes.
250 Each pass of the outer loop consists of the inner loop followed by a computation of the robustness
251 weights, which are used in the following run of the inner loop to minimise the influence of transient and
252 aberrant behaviour on the trend and seasonal components. The initial pass of the outer loop is performed
253 with all robustness weights equal to 1, followed by $n_{(0)}$ passes of the outer loop. The Kalman Smoother
254 (KS) was used to provide minimum-variance, unbiased linear estimations of observations and to impute
255 missing data to satisfy the STL (Reinsel, 1997; Durbin et al., 2012; Carslaw, 2015). Overall, statistical
256 seasonal auto-regressive and moving averages with annual seasonal components were employed.
257 Statistical analyses were carried out with SPSS 19.0.

258
259 In order to carry out seasonal analyses of data, seasons were defined according to temperature records
260 in the NH, as described previously (Hernandez-Paniagua et al., 2015): winter (December-February),
261 spring (March-May), summer (June-August) and autumn (September-November). Wind-sector analyses
262 of data were performed by defining 8 wind sectors each of 45° starting from $0^\circ \pm 22.5^\circ$. The lower bound
263 of each sector was established by adding 0.5° to avoid data duplicity. Data were assigned to a calm
264 sector when wind speed was $\leq 0.36 \text{ km h}^{-1}$ (0.1 m s^{-1}). To assess regional transport, air mass back-
265 trajectories (AMBT) were calculated using the HYSPLIT model v.4 (NOAA Air Resources Laboratory
266 (ARL); Stein et al., 2015), with the Global NOAA-NCEP/NCAR reanalysis data files on a latitude-

267 longitude grid of 2.5° , downloaded from the NOAA ARL website
268 (<http://ready.arl.noaa.gov/HYSPLIT.php>). HYSPLIT frequency plots of 96-h AMBT were constructed for
269 every 6 h during the year 2014 with an arrival altitude of 100 m above ground level.

270

271 **3. Results**

272 **3.1 Wind occurrence at the MMA**

273 The MMA is highly influenced by anti-cyclonic easterly air masses that arrive from the Gulf of Mexico,
274 especially during spring and summer (Fig. S5). Figure 2 shows the frequency count of 1-h averages of
275 wind direction by site and season within the MMA during 1993-2014. At all sites, apart from OBI, the
276 predominant wind direction is clearly E, which occurs between 35-58 % of the time depending on season.
277 Easterly air masses are augmented by emissions from the industrial area E of the MMA, which are
278 transported across the urban core and prevented from dispersing by the mountains located S-SW of the
279 MMA. On average, the highest wind speeds are observed during summer at all sites. By contrast, calm
280 winds of $\leq 0.36 \text{ km h}^{-1}$ (0.1 m s^{-1}) occurred less than 2 % of the time at all sites, most frequently in winter,
281 and least frequently in summer.

282

283 **3.2 Time-series in O_3 and O_x recorded within the MMA during 1993-2014**

284 Within the MMA, the highest O_3 mixing ratios (1-h averages) are typically observed between April-
285 September during the photochemical season, whereas the lowest values are usually recorded between
286 December-January (winter) (Fig. S6). Table S1 summarises the minimum, maximum, average (mean)
287 and median hourly O_3 mixing ratios recorded during 1993-2014. The highest O_3 mixing ratios recorded
288 were 186 ppb at GPE in 1997, 146 ppb at SNN in 2004, and 224 ppb at SNB in 2001. At OBI and STA,
289 the highest O_3 mixing ratios were both recorded on June 2, 1993: 182 ppb at 12:00 CDT at OBI, and 183
290 ppb at 13:00 CDT at STA, during the occurrence of E winds. Note that all times below are given in CDT.
291 Annual O_3 averages varied from 14 ± 14 ppb at OBI in 2001 to 32 ± 23 ppb at SNB in 1993, whereas O_3
292 annual medians ranged from 10 ppb at OBI in 2001 to 28 ppb at SNN in 1993.

293

294 Reaction with O_3 rapidly converts NO to NO_2 , and therefore mixing ratios of odd oxygen ($\text{O}_x = \text{O}_3 + \text{NO}_2$)
295 were calculated to account for O_3 stored as NO_2 for each hour during 1993-2014 at the 5 sites within the
296 MMA (Table S2; Fig. S7). Minimum values of O_x ranged from 2 ppb, observed at all sites mostly during
297 1993-2014 to 13 ppb at OBI in 2007. Maximum values of O_x ranged from 99 ppb at SNN in 2002, to 330
298 at OBI in 1993. O_x annual averages varied from 23 ± 17 ppb at SNN in 2002 to 51 ± 27 ppb at OBI and
299 at STA in 2001 and 2006, respectively, whereas O_x annual medians ranged from 21 ppb at SNB and
300 SNN, in 2001 and 2002, respectively, to 46 ppb at OBI and STA in 2001 and 2006, respectively. It is
301 clear that the highest O_3 and O_x mixing ratios were recorded when control of precursor emissions of
302 VOCs and NO_x were less stringent than subsequently.

303

304

305 **3.2 Diurnal variations in O₃ and O_x within the MMA**

306 Diurnal variations in O₃ arise from the balance between its net production and destruction. Here, O₃
307 diurnal variations were used to assess changes in the net O₃ production. Figure 3 shows daily profiles
308 by season of O₃, O_x, NO, NO₂, NO_x, and SR averaged over the 5 sites within the MMA. O₃ generally
309 dips during the morning rush hour due to titration with NO and mirrors the increase in NO₂, which occurs
310 around 07:00 in spring and summer, and around 08:00 in autumn and winter. The 1-h difference in the
311 O₃ dip derives from the change to daylight saving time during spring and summer. O₃ generally peaks
312 during the enhanced photochemical period, around 13:00 in spring, 12:00 in summer (co-incident with
313 SR), and about 14:00 in autumn and winter. Similar profiles are observed for O₃ in all seasons, being
314 negatively correlated with NO₂ ($r=0.93$ (winter) to $r=0.97$ (summer) ($p<0.05$)), due to the rapid photolysis
315 of NO₂. Diurnal cycles of O_x behave as O₃, with lowest values before the morning rush hour and the
316 largest between midday (summer) and 15:00 (winter). During daytime, O_x and O₃ diurnal cycles are
317 strongly correlated in all seasons, ranging from $r=0.97$ in winter to $r=0.99$ in autumn ($p<0.05$), which
318 suggests net O₃ production during daytime.

319

320 O₃ and O_x levels depend strongly on the photochemical processing of NO_x and VOCs emissions. To
321 assess differences in the net O₃ production from site-to-site within the MMA, O₃ and O_x amplitude values
322 (AV_d) derived from normalised daily cycles were used as proxy. The normalised daily cycles were
323 constructed by subtracting daily averages from hourly averages. Figure 4 shows normalised O₃ daily
324 cycles and Fig. S8 normalised O_x daily cycles. The lowest AV_ds both in O_x and O₃ occur in winter
325 consistent with reduced SR and low photolysis rates, while the largest ones are seen in summer. It is
326 clear that during the whole year, the largest AV_ds are recorded at sites downwind of the industrial
327 emission sources, in particular at STA, while the lowest AV_ds are observed at upwind sites. The larger
328 AV_ds at downwind sites indicate higher net O₃ production, derived from photochemical processing of air
329 masses from the E sector. The AV_ds seen at upwind sites indicate that these are less affected by
330 emissions from the largest part of the MMA and from the industrial area.

331

332 **3.3. Annual cycles of O₃ and O_x within the MMA**

333 Annual variations in O₃ and O_x are correlated positively with the seasonality of temperature, RH and SR
334 (Camalier et al., 2007; Zheng et al., 2007). Annual averages cycle for those meteorological variables, O₃
335 and O_x were constructed by averaging monthly averages for the same month during the studied period.
336 Figure 5a shows that O₃ exhibits the maxima during spring and minima in winter, with a downward peak
337 in early autumn, behaviour characteristic of tropospheric O₃ in the NH. O_x peaks in spring and dips in
338 summer, although it is evident that NO_x emissions lead to apparently similar O_x levels in winter and
339 spring despite the decrease in O₃ levels. A correlation analysis among monthly averages for both O₃ and
340 O_x with temperature, rainfall, RH and SR, revealed that the strongest relationship was between O₃ and
341 SR ($r= 0.72$, $p<0.001$; Fig. 5a), with relationship evident with O_x.

343 Seasonal amplitude values (AV_s) provide insight into inter-annual variations in the net O_3 production in
344 response to changes in precursor emissions and meteorology. The seasonal cycles in O_3 during 1993-
345 2014 were determined by filtering monthly averages with the STL technique (Cleveland et al., 1990) (Fig.
346 S9). $O_3 AV_s$ s were calculated as the difference peak-to-trough (spring peak). An average $O_3 AV_s$ of 15.1
347 ± 2.97 (1σ) ppb was calculated from 1993 to 2014 within the MMA, with the lowest $O_3 AV_s$ of 10.3 ppb
348 determined in 1998, and the largest $O_3 AV_s$ of 19.0 ppb observed in 2014. Figure 5b shows that $O_3 AV_s$
349 decreased significantly at all sites between 1993 and 1997-1998, at rates from 0.78 ppb $O_3 yr^{-1}$ at GPE
350 to 2.28 ppb $O_3 yr^{-1}$ at SNN (Fig. 5c). $O_3 AV_s$ s increased constantly ($p<0.05$) at all sites since 1998, ranging
351 from 0.90 ppb $O_3 yr^{-1}$ at GPE to 0.75 ppb $O_3 yr^{-1}$ at SNN. $O_x AV_s$ s exhibited no discernible trends at all
352 sites for the whole studied period, although, SNN show a significant ($p<0.05$) decline during 1993-2001
353 (1.5 ppb yr^{-1}) and at STA show an increase during 2004-2010 (1.3 ppb yr^{-1}). The trends in O_x follow those
354 observed for NO_x at SNN and STA during 1993-2014, which indicates that nearby industrial emissions
355 have a significant contribution on the observed O_x levels within the MMA.

357 **3.4. Long-term trends in O_3 and O_x within the MMA during 1993-2014**

358 Quantifying the absolute changes in ground-level O_3 in response to trends in its precursor emissions is
359 crucial to evaluate the impacts of air quality control (Parrish et al., 2009; Simon et al., 2015). The growing
360 economy within the MMA has increased O_3 precursor emissions from point and area sources, due to the
361 limited emissions control programs (INEGI, 2015; SDS, 2015). Moreover, predominant E-SE winds
362 throughout the year transports primary pollutants and their oxidised products downwind from the
363 industrial area, which can offset reductions in emissions from other sources. Here, to characterise
364 changes in net O_3 production during 1993-2014 within the MMA in response to changes in its precursor
365 emissions, long-term trends for daytime (06:00-18:00 CDT) O_3 and O_x measurements were derived by
366 averaging data in seasonal periods. Seasonal averaging was used to minimise variability inherent in
367 longer-term averages and the de-seasonalisation process avoids confounding overall trends, especially
368 when seasons exhibit opposite trends. (Parrish et al., 2009).

370 Figure 6 shows seasonal trends in O_3 within the MMA, and Table 3 summarises the parameterisation of
371 the trends. Significant increases ($p<0.1$) in O_3 are observed at all sites, apart from STA, in spring and
372 summer, while in autumn, O_3 increases significantly only at SNN and SNB. The increases in O_3 range
373 from 0.26 ppb yr^{-1} in spring at OBI to 0.47 ppb yr^{-1} in summer at SNN. Overall, the lowest O_3 growth rates
374 are observed at the urban background GPE site, whereas the largest ones are at the industrial SNN site.
375 It is worth noting that only SNN and OBI exhibit significant increases in autumn, despite a decrease in
376 the frequency of high wind speeds (>20 km h^{-1}). The existence of significant trends at all sites during
377 spring-summer, except for OBI, is consistent with the downwind transport of industrial emissions and the
378 high frequency of photochemical processed air masses with NE-S-SE origin, where the industrial area
379 is located (Fig. S10).

381 Seasonal trends in O_x are shown in Fig. 7, with the parameters of the trends listed in Table 3. Consistent
382 with the seasonal O_3 trends observed, significant increases ($p<0.1$) in O_x within the MMA are determined
383 in spring at all sites except for STA, and range from 0.02 ppb yr^{-1} at OBI to 0.67 ppb yr^{-1} at SNB. It is
384 worth noting that the industrial SNN and SNB sites show significant increases in O_x in all seasons, with
385 the lowest growth rates in winter and the largest in summer and spring, respectively. Moreover, STA
386 exhibits the only significant decrease in O_x of 0.63 ppb yr^{-1} during winter. As for O_3 , the O_x increasing
387 trends are consistent with the transport of primary emissions during the high occurrence of NE-E-SE air
388 masses at $WS > 10 \text{ km h}^{-1}$, which is highlighted during the photochemical season (April-September).
389 Furthermore, the small shift in wind direction at STA to NW during winter coincides with the only observed
390 decrease in net O_3 production within the MMA, which confirms that O_3 precursors are emitted E of the
391 MMA. This also makes evident that increasing upwind industrial emissions have offset reductions in
392 emissions from on-road sources as revealed by the decline in NO_x evident at OBI.

394 3.5 Comparison of MMA O_3 and O_x weekly profiles with those at MCMA and GMA

395 O_3 production varies from city-to-city in response to local NO_x and VOCs emissions. Assessment of
396 weekly profiles of O_3 and O_x may provide insights of the geographic response in net O_3 production to
397 diurnal variations in precursor emissions. Hourly O_3 and O_x averages were used to construct weekday
398 and weekend average profiles for the MCMA from 1993 to 2014, and for the GMA from 1996 to 2014.
399 Figure 8 compares weekly O_3 and O_x profiles by season within the MMA with those for the MCMA and
400 GMA. In each case, and consistent with observations in other major urban areas of NA, the lowest O_3
401 mixing ratios occur during the morning rush hour due to O_3 titration with NO emitted from on-road
402 sources, whereas peak values of O_3 are apparent after mid-day during periods of enhanced SR
403 (Stephens et al., 2008; Jaimes-Palomera et al., 2016). It should be noted that the peak value of O_3 for
404 the GMA in winter and spring occurs an hour or so earlier than for the MMA and MCMA, which is
405 consistent with higher VOC/ NO_x emissions ratios at the GMA (Kanda et al., 2016). As might be
406 anticipated, larger AV_d of $76.9 \pm 1.6 \text{ ppb } O_3$ are observed for the MCMA than for the GMA (46.1 ± 1.0
407 ppb O_3) and MMA ($37.6 \pm 0.4 \text{ ppb } O_3$), related to the levels of emissions of the O_3 precursors. The O_x
408 profiles show a trough during the morning rush hour and a peak between 12:00 and 14:00 at all urban
409 areas. Despite large variations between weekday and weekend NO_x mixing ratios at the 3 urban areas
410 as shown in Fig. 8, no significant differences ($p>0.05$) in O_3 and O_x are observed at any of the
411 metropolitan areas between O_3 and O_x weekends and weekdays AV_{ds} .

412 Stephens et al. (2008) suggested that the most plausible explanation for the lack of weekend O_3 effect
413 at MCMA during 1987-2007, is that weekday O_3 production is limited by VOCs and inhibited by NO_x .
414 Therefore, the very similar levels O_3 observed during weekdays and weekends can be explained by
415 simultaneous decreases in NO_x and VOCs emissions and the resulting effects on net O_3 production.
416 Similarly, a VOC-limited O_3 production regime was reported for the MMA by Sierra et al. (2013), whereas
417 Kanda et al. (2016) reported that at the GMA the O_3 production lies in the region between VOC- and

419 NO_x-sensitivity. Therefore, it can be hypothesised that simultaneous decreases in emissions of NO_x and
420 VOCs during weekends at the GMA and MMA explain the similarity in behaviour in O₃ and O_x as at the
421 MCMA. Indeed, Wolff et al. (2013) reported that at several urban areas of the US, similar or even higher
422 ($\pm 5\%$) O₃ levels during weekdays than at weekends were due to lower O₃ precursor emissions over
423 weekends. Furthermore, the number of sites in the US that exhibited a weekend effect decreased from
424 ca. 35 % to less than 5 % from 1997-1999 to 2008-2010, which was attributed to an increase in the
425 VOC/NO_x emission ratio derived from a greater decline in NO_x than in VOCs emissions, mostly driven
426 by reductions from on-road sources. A change to a NO_x-limited O₃ production regime during weekends
427 at the three urban areas seems unlikely, since this would result in lower O₃ levels during weekends,
428 which is not observed at any of the studied urban areas (Torres-Jardon et al., 2009).

429

430 3.6 Long-term trends at MCMA, GMA and MMA from 1993 to 2014

431 The high mixing ratios of O₃ observed typically at the 3 largest urban areas in Mexico have motivated
432 the introduction of control strategies to decrease emissions of the O₃ precursors, NO_x and VOCs. The
433 success of the control strategies implemented can be evaluated by assessing trends in O₃ and O_x. As
434 for the MMA, seasonal trends in O₃ and O_x within the MCMA and GMA were calculated from daytime
435 measurements. Figure 9 shows a comparison of inter-annual trends in O₃ and O_x at the 3 urban areas
436 in Mexico, and Table 4 lists the parameters of the trends. Overall, during 1993-2014, daytime O₃ at the
437 MCMA decreased significantly ($p<0.05$) by 1.15 ppb yr⁻¹ (2.04 % yr⁻¹), and increased at the MMA by 0.22
438 ppb yr⁻¹ (0.84 % yr⁻¹); at the GMA no discernible trend was observed during 1996-2014. For daytime O_x
439 at the MCMA and GMA during the same periods, significant decreases ($p<0.05$) of 1.87 and 1.46 ppb yr⁻¹
440 were determined, respectively, while the MMA does not exhibit a significant change. At the MCMA, the
441 overall trends in O₃ and O_x are strongly driven by their wintertime decreases of 1.62 and 2.47 ppb yr⁻¹,
442 respectively; whereas at the MMA, the annual growth in O₃ is driven by increases in spring and summer
443 of 0.32 and 0.27 ppb yr⁻¹, respectively. Although, at the MMA, an increase in O_x of 0.28 ppb yr⁻¹ is
444 observed only during summer, the overall O_x trend is strongly affected by the non-significant trends in
445 the other seasons. It is worth nothing that at the GMA, the overall decrease in O_x of 1.46 ppb yr⁻¹ is
446 similar for all seasons, which range between 1.40 ppb yr⁻¹ (autumn) and 1.89 ppb yr⁻¹ (spring).

447

448 The overall trends in net O₃ production during 1993-2014 at the MCMA and GMA are consistent with the
449 significant ($p<0.05$) annual decreases in NO_x of 1.21 and 1.25 ppb yr⁻¹, respectively (Fig. 10). By contrast,
450 while average NO_x levels have increased annually at the MMA at 0.33 ppb yr⁻¹ ($p<0.05$), the average net
451 O₃ production has remain steady. Either the non-linear response in O_x to the changes in NO_x in an
452 environment of high NO_x mixing ratios (>60 ppb) displace the chemical equilibrium to favour NO as the
453 dominant component of NO_x which does not account for the levels of O_x (Clapp and Jenkin, 2001). Or
454 the O_x trends derived from the combined data set for the MMA do not represent local observed trends,
455 because a compensating effect between O_x reductions and increases.

456

457 **3.7 Compliance with the 1-h and 8-h Mexican Standards for O₃ within the MMA**

458 Between 1993 and 2014, there were two official standards for maximum permitted mixing ratios of O₃ in
459 Mexico: i) a running 8-h average of 80 ppb, not to be exceeded more than 4 times per calendar year,
460 and ii) a 1-h average of 110 ppb (NOM-020-SSA1-1993). Since 19 Oct 2014, the maximum permitted O₃
461 levels were lowered to a running 8-h average of 70 ppb and a 1-h average of 95 ppb, (NOM-020-SSA1-
462 2014). However, because both standards are applicable for whole calendar years, the old permitted O₃
463 levels were used in this study to determine the number of annual exceedances to both O₃ standards.
464 Figure 11 shows that within the MMA, the O₃ 1-h average and the running 8-h standards were frequently
465 exceeded (INE, 2011; SEMARNAT, 2015). The largest number of exceedances occurs at STA, followed
466 by SNB, GPE and OBI, whereas the fewest breaches are observed at SNN markedly since 2004.
467 However, there have been 3 periods of clear decreased exceedances at all sites (except STA in 2014),
468 during 1994-1995, 1999-2000, and 2012-2013, which are consistent with marked changes in the national
469 GDP during economic recessions in Mexico (Fig. S11a). However, although, national GDP exhibits a
470 notable decrease during the 2008-2009 global economic recession, only in 2009 do the O₃ annual
471 exceedances within the MMA seem to follow (Fig. S11b).

472
473 Therefore, if O₃ levels continue to increase within the MMA, as determined in the long-term trend
474 assessment, an increase also in peak O₃ mixing ratios is likely to occur. Hence, to analyse changes in
475 peak O₃, daily maxima 1-h averages from 1993 to 2014 were used to determine seasonal trends in peak
476 levels. Figure 12 shows trends in 1-h daily maxima and Table 5 list the parameters of the trends. Daily
477 maxima O₃ 1-h averages have increased significantly ($p<0.05$) in spring and summer at all sites, except
478 for STA, and also in autumn at the industrial sites SNN and SNB. The largest increases in the daily
479 maxima are seen at SNN, where similar increases between 0.85 and 0.93 ppb yr⁻¹ are determined
480 between spring and autumn. SNB exhibits slightly lower growth rates in spring and summer, but a large
481 difference in autumn.

482
483 We have shown that predominantly E-SE winds transport photochemically processed air mases to SNN
484 and SNB during spring-summer leading to the observed exceedances. Moreover, the change in the wind
485 occurrence in autumn at SNB leads to a lower growth rate than at SNN, where the calmest winds during
486 the whole year drive the largest increase interpreted to be due to the photochemical processing of
487 precursors emitted locally. The GPE and OBI sites exhibit increases only in spring and summer, with the
488 lowest increases of all sites determined at OBI of 0.48 ppb yr⁻¹ in spring, which contrasts with the largest
489 increase at OBI during the same season. However, such increases are consistent with an increase in
490 the occurrence of NE and E air masses at high speeds (>10 km h⁻¹) during spring-summer. STA shows
491 a significant decrease in the maxima daily O₃ 1-h averages of 0.35 ppb yr⁻¹ in winter, which is consistent
492 with an increase in the occurrence of NW air masses at WS < 5 km h⁻¹, loaded with high NO_x mixing
493 ratios (50 ppb) that promote the O₃ titration.

495 **4. Discussion**

496 **4.1 Strategies for air quality control in Mexico**

497 The Mexican environmental authorities have focused largely on improving the air quality within the
498 MCMA since 1986, by implementing numerous strategies to control primary emissions, but have paid
499 less attention to other large metropolitan areas in Mexico (PICCA, 1990; ProAire-MCMA, 2011). Control
500 measures have been designed based on NAEI and local emission inventories data, which possess
501 significant uncertainties (Arriaga-Colina et al., 2004; Velasco et al., 2007; Kanda et al., 2016). However,
502 despite these uncertainties, the emission control strategies have helped to reduce O₃ levels within the
503 MCMA since 1991-1992 (ProAire-MCMA, 2001). Here, we describe the most effective measures
504 introduced to control O₃ precursor emissions within the MCMA, and then discuss potential benefits of
505 implementing such measures within the MMA.

506

507 From 1993 to 2014, NO_x levels within the MCMA decreased at a rate of around 1.2 ppb yr⁻¹ (1.6 % yr⁻¹)
508 as determined from ground-based measurements. This decline is remarkably consistent with the
509 decrease during 2005-2014 in the NO₂ column over the MCMA of 1.6 % yr⁻¹ reported by Duncan et al.
510 (2016). The decrease in NO_x has been driven largely by reductions in emissions from on-road sources,
511 in response to the introduction of mandatory 3-way catalytic converters in new vehicles since 1993
512 (NOM-042; SEMARNAT, 1993), and by the introduction of a no driving day and more stringent exhaust
513 emissions inspection programs for private cars since 1989 (NOM-041; SEMARNAT, 1993). The NO_x
514 reduction measures also required public transport vehicles to switch from petrol to LP gas fuelled
515 engines, new road corridors were designed for improving the intracity transport and the public transport
516 fleet was renewed (ProAire-MCMA, 2001). For industrial sources, the switch from fuel oil to LP gas fuel,
517 relocation of highly polluting industries away from the MCMA, and implementation of regular inspections
518 programs of NO_x emission for industrial and area sources were also implemented (ProAire-MCMA,
519 2001).

520

521 While the outlook for NO_x levels within the MCMA is clear, studies of VOCs levels have reported no
522 concluding trends. For instance, Arriaga-Colina et al. (2004) reported a decrease in VOCs of around 10
523 % from 1992 to 2001 over the N MCMA, while Garzón et al. (2015) reported that on average VOCs
524 increased over most of the MCMA between 1992-2002 but decreased by 2.4 ppb yr⁻¹ between 2002-
525 2012. However, the decrease in VOCs from 2002 to 2012 reported by Garzón et al. (2015) is consistent
526 with a reduction in light alkanes and aromatics levels during the morning rush hour reported by Jaimes-
527 Palomera et al. (2016). Continuous measurements of VOCs have been introduced recently by the MCMA
528 government, which precludes an assessment of VOCs long-term trends. The measures implemented to
529 control VOCs emissions from on-road sources have included the reformulation of petrol with the
530 reduction of highly reactive VOCs and addition of oxygenated compounds, and fitting of 3-way catalytic
531 converter in all new vehicles (NOM-042; SEMARNAT, 1993; ProAire-MCMA, 2001). For area sources,
532 control measures include the introduction of vapour emissions control systems at petrol stations and

533 introduction of a LP gas leak detection program for the distribution network (ProAire-MCMA, 2011). As
534 for NO_x, industrial VOCs emission sources have been subject to regular emissions inspections and
535 relocation of the most significant emitters (ProAire-MCMA, 2011).

536

537 Therefore, the moderate success on controlling O₃ levels within the MMA can be interpreted as the
538 implementation of effective controls measures on VOCs and NO_x emissions. Thus, a comparison
539 between VOCs and NO_x trends derived from the NAEI and local emissions inventories with those
540 determined from ground-levels measurements can provide insight into further improvements in
541 decreasing O₃ levels not only within the MCMA but also at other large metropolitan areas in Mexico.
542 Within the MCMA, the NAEI NO_x emissions trends are consistent with the decrease determined from
543 ground-based measurements made by SIMAT, but the MCMA local inventory trends disagree with the
544 SIMAT trends (Fig. S1 and Fig. 10). For VOCs, the NAEI and the MCMA inventories oppose measured
545 trends in VOCs during 1993-2001 (Arriaga-Colina et al., 2004; Garzón et al., 2015). This can be
546 explained by underestimates of VOC emissions within the MCMA of a factor of 2-3 (Arriaga-Colina et al.,
547 2004; Velasco et al., 2007). Such discrepancies suggest that, significant improvements in NO_x and VOCs
548 emissions inventories are still required to better inform O₃ control strategies.

549

550 **4.2 Ground-level O₃ and O_x variations within the MMA**

551 The O₃ and O_x diurnal variations result from the particular chemical environment and meteorological
552 conditions at each monitoring site within the MMA. Thus, the largest O₃ and O_x mixing ratios, except for
553 OBI, are observed typically for air masses from the E and SE wind sectors, whereas at OBI, the largest
554 O₃ and O_x values are recorded during the occurrence of NE and E air masses. It is clear that short-range
555 transport and large upwind emissions of O₃ precursors from the industrial area dominate the MMA
556 (SEMARNAT, 2006, 2011, 2014; SDS, 2015). This is underlined at OBI with the highest values of O_x
557 where the predominant wind direction is NE, consistent with the transport of emissions from the industrial
558 area located NE, and photochemical processing of air masses (Carrillo et al., 2017). The daily cycles of
559 O₃ determined within the MMA are consistent with those reported for Los Angeles (VanCuren, 2015),
560 and Toronto (Pugliese et al., 2014). At Toronto, the O₃ maxima were enhanced by the arrival of
561 photochemical processed air masses transported from polluted wind sectors, and decreased during clear
562 air masses. This behaviour is similar to that observed within the MCMA with enhanced O₃ maxima during
563 the occurrence of E-SE (polluted) and decreased levels when SW-W (relatively clean) air masses
564 occurred.

565

566 **4.3. Origin of the O₃ annual cycles within the MMA**

567 The O₃ annual cycles within the MCMA are consistent with the spring maxima and winter minima
568 characteristic of the US southeast regions (Strode et al., 2015), and follow the O₃ cyclic pattern at NH
569 mid-latitudes (Monks 2000; Vingarzan, 2004). However, they are different to O₃ annual cycles reported
570 for the US west coast regions, particularly in California, where the maxima in the cycle occurs between

571 June-August, driven the local influence of precursor emissions upon O₃ production and photochemical
572 conditions (Vingarzan, 2004; Strode et al., 2015). The recurrent downward spikes in the O₃ annual cycles
573 within the MMA between July-August result from high wind speeds (>10 km h⁻¹ on average) that disperse
574 O₃ precursors and increase the boundary layer height (ProAire-MMA, 2008). The peak in O₃ observed
575 in September is characteristic of humid regions, and can be ascribed to an increase in OH radicals
576 derived from the increment in RH during the rainy season (Lee et al., 2014). A marked increase in RH
577 within the MMA during September is consistent with the increase in O₃ observed as reported by Lee et
578 al. (2014). Over the mid-western and eastern US regions, that O₃ peak has become less noticeable since
579 2000 (Zheng et al., 2007).

580
581 The annual variability in O₃ within the MMA is strongly coupled to the economic conditions (GDP) in
582 Mexico. For instance, the economic crisis of 1994-1996 caused a marked reduction in industrial
583 emissions of VOCs and NO_x, which is confirmed by the significantly decrease in O₃ annual variations at
584 all sites within the MMA (Tiwari et al., 2014; INEGI, 2016). During the global economic recession of 2008-
585 2009, Castellanos and Boersma (2012) reported a reduction of 10-30 % in tropospheric NO₂ over large
586 European urban areas, which is consistent with a faster decline of 8 ± 5 % yr⁻¹ in the NO₂ column density
587 during the same period for US urban regions (Russell et al., 2012). Increases in the NO₂ column density
588 over the MMA as reported by Duncan et al. (2016) are explained by the gradual recovery of the economy
589 since 1997 in Mexico. Moreover, increases in O₃ precursor emissions and in annual variability observed
590 within the MMA are consistent with such economic growth. This explains clearly the opposite trends in
591 O₃ annual variations before and after the economic crisis within the MMA, with the lowest changes seen
592 at the urban GPE site and the greatest ones detected for the SNN industrial site.

593
594 **4.4 Increasing O₃ and O_x levels within the MMA**
595 Ground-based measurements made during 1993-2014 reveal significant ($p<0.05$) increases in NO_x
596 within the MMA at all sites, apart from OBI, which exhibits a significant decrease (Fig. 13). Overall, the
597 NO_x increase within the MMA of 1.24 % yr⁻¹ (0.33 ppb yr⁻¹) during 1993-2014 is larger than the increase
598 in the NO₂ column density over the MMA of around 0.78 % yr⁻¹ during 2005-2014 reported by Duncan et
599 al. (2016), although both indicate a significant increase in the NO_x levels at least since 2005. The largest
600 increases in NO_x correspond to industrial sites, SNN (0.51 ppb yr⁻¹) and SNB (0.74 ppb yr⁻¹), which is
601 interpreted as a response to growing industrial activity, in combination with flexible emission regulations
602 within the MMA (INEGI, 2016). The influence of industrial emissions upon O₃ at the MMA becomes
603 evident by the lowest NO_x growth rate observed at GPE of 0.19 ppb yr⁻¹, since OBI has few occurrences
604 of air masses transporting pollutants from the largely industrialised areas throughout the year (Fig. 2).
605 By contrast, the NO_x decrease at OBI of -0.40 ppb yr⁻¹ arises from decreases in emissions from on-road
606 sources (SDS, 2015). The large growth rates in O₃ and NO_x at SNN and SNB are explained by increasing
607 emissions of O₃ precursors from a growing number of industries and the urban development E of the
608 MMA. The most likely explanation for the O₃ increase at OBI is a reduced titration effect by decreasing

609 NO_x levels in combination with the non-linear response in O₃ production to decreasing NO_x emissions
610 under the VOC-sensitive MMA airshed (Sierra et al., 2013; Menchaca-Torre et al. 2015).

611
612 The O₃ increasing trends within the MMA are opposite to those reported by Sather and Cavender (2016)
613 at 4 South Central US urban areas, where NO_x and VOCs decreased by 31-70 % and 43-72 % during
614 1983-2015, respectively, resulting in a reduction between 18-37 ppb O₃ in the 8-h averages. The O₃
615 response to NO_x decreases at OBI is similar to that observed in central London during 1996-2008 (Bigi
616 and Harrison, (2010), and at four urban areas in Japan during 1990-2010, explained by the decrease of
617 the NO titration effect (Akimoto et al., 2015). This suggests that controlling VOCs emissions may lead to
618 a decrease in the net O₃ production, whereas decreases in NO_x may not have significant effects on O₃
619 production or even increase the O₃ levels due existence of a VOC-limited environment within the MMA
620 (Sierra et al., 2013, Carrillo et al., 2017).

621
622 The O_x long-term trends during 1993-2014 within the MMA were consistent with those for O₃ at all sites.
623 Decreases in NO_x and O₃ observed between 1994-1996 were the response to the economic crisis during
624 the same period in Mexico, when the DGP decreased by 5.9 % providing additional evidence of the
625 dominant role of industries within the MMA. Consistent with economic indicators, annual averaged petrol
626 sales in the Nuevo Leon state in 1995 decreased by 2.4 % in relation to 1994, but increased linearly from
627 1996 to 2008 at an approximate rate of 98,800 m³ petrol yr⁻¹ ($r = 0.90$) (Fig. S12) (SENER, 2015). As for
628 petrol sales, registered vehicles in Nuevo Leon show significant variations between 1993-1996, but
629 increase linearly since 1997 at a rate of around 100,000 vehicles yr⁻¹ ($r=0.99$). This confirms that despite
630 the annual growth in the vehicular fleet, the fitting of 3-way catalyst technology and reformulation of petrol
631 introduced in 1997 has controlled on-road primary emissions (ProAire-MCMA, 2001) The decreases in
632 NO_x observed at OBI and at all sites during the occurrence of SW-W-NW air masses reflect that if
633 applied, stricter emissions controls such as those for on-road sources can lead to a significant abatement
634 in primary emissions. It is clear that the industrial sources must be subject to similar emission control
635 measures as those implemented within the MMA for effectively reducing the O₃ levels.

636
637 **4.5 The opposite O₃ trends at Mexican urban areas**
638 The comparison of O₃ and O_x trends at MMA, GMA and MCMA reveals different emission trends at each
639 of the studied cities. The trends in O₃ reported in this study for the MCMA, agree with the reduction of
640 20 ppb O₃ during 1991-2011 for the MCMA (Jaimes et al., 2012), and with the reduction of 8 ppb O₃
641 during 2000-2011 for the MMA (Benítez-García et al., 2014). At the GMA, the no trend status in O₃
642 determined here is in contrast with the increase of 12 ppb O₃ during 2000-2011 (Benítez-García et al.,
643 2014), which is due to the different periods assessed in the latter. Decreases in O₃ in US urban areas
644 arise from effective control of O₃ precursor emissions (Strode et al., 2015), which has occurred at the
645 MCMA. By contrast, O₃ levels increased in urban areas of Japan by 0.22-0.37 ppb yr⁻¹ (Akimoto et al.,
646 2015), and in the Greater London by 0.5 ppb yr⁻¹ (Bigi and Harrison, 2010), due to faster declines in NO_x

647 than in VOCs and are slightly similar that observed in O_3 averages for the MMA (0.20 ppb yr^{-1}), where
648 average NO_x levels have increased and also likely VOCs.

649

650 Trends in net O_3 production can be interpreted as the response to trends in its precursors, which also
651 respond to implemented policies to control their emissions and to economic factors. Figure 10 shows
652 that NO_x decreased significantly within the MCMA (1.57 % yr^{-1}) and the GMA (1.83 % yr^{-1}) during 1993-
653 2014 and 1996-2014, respectively, but increased within the MMA (1.83 % yr^{-1}) during 1993-2014. Such
654 NO_x trends are within the range of the trends in the NO_2 column density reported by Duncan et al. (2016)
655 in Table S9, which reveals an increase of 0.78 ± 1.12 % yr^{-1} for the MMA, but decreases of 1.82 ± 0.84
656 % yr^{-1} for the GMA and of 0.10 ± 1.67 % yr^{-1} for the MCMA, all during 2005-2014. To date, long-term
657 trends in VOCs have only been reported only the MCMA with an average decrease of ca. 2.4 ppb yr^{-1}
658 since 2002, mostly in propane, ethanol and acetone (Garzón et al., 2016), while there are no studies of
659 long-term trends in VOCs within the MMA and the GMA.

660

661 It is clear that O_3 and O_x decreases within the MCMA have been driven by reductions in NO_x and VOCs
662 emissions, and that the implemented strategies described in Sect. 4.1 have proved to be effective in
663 controlling primary emissions. By contrast, growing industrial emissions within the MMA must be subject
664 to stringent controls to abate O_3 levels. In the GMA, where the industrial activity is lower than at the
665 MCMA and MMA (Kanda et al., 2016), the policies introduced at national scale for controlling on-road
666 sources emissions have resulted in the decrease of NO_x emissions and in the stabilisation of O_3 levels.
667 Finally, the results presented here demonstrate the merits of the assessment and analysis of long-term
668 O_3 levels, which can be used by environmental authorities to revise and to redesign programs and
669 policies to improve air quality. Continuing with ground-based O_3 and NO_x monitoring is strongly
670 recommended to better understand the response further changes in local and regional O_3 levels to
671 changes in primary emissions. Monitoring of VOCs at the GMA and MMA is also recommended to as
672 the VOCs emissions data reported in the NAEI possess significant uncertainties.

673

674 **5. Conclusions**

675 Diurnal and annual cycles, and long-term trends in O_3 and O_x within the MMA, are interpreted as
676 response to changes in NO_x and VOCs emissions, photochemistry and meteorology. Continuous high-
677 frequency and high-precision O_3 and NO_x data recorded during 1993-2014 at 5 sites within the MMA
678 and at 29 sites within the MCMA, and during 1996-2014 at 10 sites within the GMA, were used to
679 calculate long-term trends. Within the MMA, the greatest mixing ratios in O_3 were recorded during E and
680 SE winds, at sites downwind of significant precursors from industrial sources. By contrast, the lowest O_3
681 mixing ratios were recorded at SNN, and for all sites were observed for the W and SW sectors, where
682 air masses travel from central Mexico over 100-300 km of semi-arid region sparsely populated. Maximum
683 daily 1-h values of O_3 and O_x increased significantly at GPE, SNN and SNB, owing to increasing

684 emissions of precursors, while at OBI increasing O₃ and decreasing O_x trends arise from the non-linear
685 response to decreasing NO_x emissions from on-road sources.

686

687 Annual cycles in O₃ at all sites peak in spring and through in winter, with a downward spike during
688 summer caused by high winds that disperse O₃, and increase the boundary layer height. Decreases in
689 O₃ precursor emissions during the economic crisis experienced in Mexico between 1994-1996, caused
690 significant decline trends O₃ annual variations from 1993 to 1997 or 1998, depending on site, followed
691 by significant increases derived from the recovery of the economy. The dominant role of industrial
692 sources on O₃ precursor levels within the MMA was evident at the industrial site SNN during the 1994-
693 1996 economic crisis.

694

695 At all metropolitan areas studied, O₃ and O_x levels showed no significant differences between weekdays
696 and weekend, although an earlier occurrence of the O₃ peak at the GMA was detected, ascribed to larger
697 VOCs/NO_x emission ratio. The lack of the weekend effect was attributed to weekday O₃ production being
698 limited by VOCs, whereas increases in the VOC/NO_x ratio during weekends in response to reduced
699 emissions from mobile sources resulted in similar O₃ mixing ratios that during weekdays. Larger AV_{ds}
700 during weekdays and weekends were seen at MCMA than at GMA and MMA related to the relative
701 emissions of the O₃ precursors.

702

703 Significant seasonal trends in O₃ and O_x during spring were observed at all sites, apart from STA,
704 whereas industrial sites exhibited significant increases for O_x in all seasons. The largest increases in O₃
705 and O_x were observed during the occurrence of NE-E-SE air masses. The only significant decrease in
706 O_x at STA was related to the NW wind occurrence during winter. NO_x mixing ratios increased significantly
707 at all sites, except at OBI, due to the dominant role of industrial sources on NO_x levels. The overall
708 significant increasing trend of 0.22 ppb O₃ yr⁻¹ within the MMA contrasts within a significant decreasing
709 trend of 1.15 ppb O₃ yr⁻¹ within the MCMA during 1993-2014, whereas a non-significant trend is evident
710 within the GMA during 1996-2014. At the MCMA and GMA, the overall O_x trends reflect the trends in O₃
711 precursors. According to the long-term trends in O₃ for the MMA, the number of exceedances of the air
712 quality standards will very likely increase as result of increasing precursor emissions. The moderate
713 mitigation of O₃ levels within the MCMA, derived from measures implemented to control emissions from
714 on-road, industrial and area sources, emphasises the need for more stringent control of emissions mostly
715 from industrial sources within the MMA in order to improve air quality. Finally, comparison between
716 emission inventories estimates of NO_x and VOCs with ground-based measurements, indicate that
717 significant reductions in uncertainties are required to better inform air quality policies.

718

719 **6. Acknowledgments**

720 This research was supported by Tecnológico de Monterrey through the Research Group for Energy and
721 Climate Change (Grant 0824A0104 and 002EICIR01). Grateful acknowledgements are made to the

722 Secretariat for Sustainable Development of the Nuevo Leon State, the Secretariat for the Environment
723 of Mexico City and the Secretariat for the Environment and Territorial Development of the Jalisco State
724 for the public domain records. We gratefully thank the NOAA Air Resources Laboratory (ARL) for access
725 to the HYSPLIT model and READY website (<http://www.ready.noaa.gov>), and Dr. Sigfrido Iglesias for
726 providing the imputed O₃ and NO_x data for the MMA time-series. We are also grateful to Professor Paul
727 Monks and Professor Richard Derwent for encouraging comments on an earlier version of the
728 manuscript.

729

730 **7. References**

731 Akimoto, H., Mori, Y., Sasaki, K., Nakanishi, H., Ohizumi, T., and Itano, Y.: Analysis of monitoring data
732 of ground-level ozone in Japan for long-term trend during 1990-2010: Causes of temporal and spatial
733 variation, *Atmos. Environ.*, 102, 302-310, doi:10.1016/j.atmosenv.2014.12.001, 2015.

734 Arriaga-Colina, J. L., West, J. J., Sosa, G., Escalona, S. S., Ordunez, R. M., and Cervantes, A. D. M.
735 Measurements of VOCs in Mexico City (1992–2001) and evaluation of VOCs and CO in the emissions
736 inventory, *Atmos. Environ.*, 38, 2523-2533, doi:10.1016/j.atmosenv.2004.01.033, 2004.

737 Atkinson, R.: Atmospheric chemistry of VOCs and NOx. *Atmos. Environ.*, 34, 2063-2101,
738 doi:10.1016/S1352-2310(99)00460-4, 2000.

739 Benítez-García, S. E., Kanda, I., Wakamatsu, S., Okazaki, Y., and Kawano, M.: Analysis of criteria air
740 pollutant trends in three Mexican metropolitan areas, *Atmosphere*, 5, 806-829,
741 doi:10.3390/atmos5040806, 2014.

742 Bigi, A., and Harrison, R. M.: Analysis of the air pollution climate at a central urban background site,
743 *Atmos. Environ.*, 44, 2004-2012, doi:10.1016/j.atmosenv.2010.02.028, 2010.

744 Boersma, K. F., Jacob, D. J., Bucsela, E. J., Perring, A. E., Dirksen, R., van der A, R. J., Yantosca, R.
745 M., Park, R. J., Wenig, M. O., Bertram, T. H., and Cohen, R. C.: Validation of OMI tropospheric NO₂
746 observations during INTEX-B and application to constrain NOx emissions over the eastern United States
747 and Mexico, *Atmos. Environ.*, 42, 4480-4497. doi:10.1016/j.atmosenv.2008.02.004, 2008.

748 Butler, T. M., Stock, Z. S., Russo, M. R., Denier Van Der Gon, H. A. C., and Lawrence, M. G.: Megacity
749 ozone air quality under four alternative future scenarios, *Atmos. Chem. Phys.*, 12, 4413-4428,
750 doi:10.5194/acp-12-4413-2012, 2012

751 Camalier, L., Cox, W., and Dolwick, P.: The effects of meteorology on ozone in urban areas and their
752 use in assessing ozone trends, *Atmos. Environ.*, 41, 7127-7137, doi: 10.1016/j.atmosenv.2007.04.061,
753 2007.

754 Carrillo-Torres, E. R., Hernández-Paniagua, I. Y., and Mendoza, A.: Use of Combined Observational-
755 and Model-Derived Photochemical Indicators to Assess the O₃-NO_x-VOC System Sensitivity in Urban
756 Areas. *Atmosphere*, 8, 22, doi:10.3390/atmos8020022, 2017.

757 Carslaw, D. C., and Ropkins, K.: openair - An R package for air quality data analysis, *Environ. Model.*
758 *Soft.*, 27-28, 52-61, doi:10.1016/j.envsoft.2011.09.008, 2012.

759 Carslaw, D. C.: The openair manual - open-source tools for analysing air pollution data, Manual for
760 version 1.1-4, King's College London, 2015.

761 Castellanos, P. and Boersma, K. F.: Reductions in nitrogen oxides over Europe driven by environmental
762 policy and economic recession, *Sci. Rep.*, 2, doi:10.1038/srep00265, 2012.

763 Clapp, L. J., and Jenkin, M. E.: Analysis of the relationship between ambient levels of O₃, NO₂ and NO
764 as a function of NO_x in the UK. *Atmospheric Environment*, 35, 6391-6405, doi: 10.1016/S1352-
765 2310(01)00378-8, 2001.

766 Cleveland, R. B., Cleveland, W. S., McRae, J., and Terpenning, I.: STL: A seasonal-trend decomposition
767 procedure based on Loess, *J. Off. Stats.*, 6, 3-33, 1990.

768 Dentener, F., Stevenson, D., Cofala, J., Mechler, R., Amann, M., Bergamaschi, P., Raes, F., and
769 Derwent, R.: The impact of air pollutant and methane emission controls on tropospheric ozone and
770 radiative forcing: CTM calculations for the period 1990-2030, *Atmos. Chem. Phys.*, 5, 1731-1755,
771 doi:10.5194/acp-5-1731-2005, 2005.

772 Duncan, B. N., Lamsal, L. N., Thompson, A. M., Yoshida, Y., Lu, Z., Streets, D. G., Hurwitz, M. M., and
773 Pickering, K. E.: A space-based, high-resolution view of notable changes in urban NO_x pollution around
774 the world (2005–2014), *J. Geophys. Res.*, 121, 976–996, doi:10.1002/2015JD024121, 2016.

775 Durbin, J., and Koopman, S. J.: *Time Series Analysis by State Space Methods*, Oxford University Press,
776 Oxford UK, 2nd Edition, 2012.

777 EPA (Environmental Protection Agency US): Compilation of Air Pollution Emission Factors (AP-42),
778 Volume I: Stationary Point and Area Sources, available at: <https://www.epa.gov/air-emissions-factors-and-quantification/ap-42-compilation-air-emission-factors>, last access: 14 Jan 2017, 1995.

780 EPA (Environmental Protection Agency US): User's Guide to MOBILE6.1 and MOBILE6.2: Mobile
781 Source Emission Factor Model, available at: <https://www3.epa.gov/otaq/models/mobile6/420r03010.pdf>, last access: 16 Jan 2017, 2003.

783 EPA (Environmental Protection Agency US): Air quality trends, available at: <https://www.epa.gov/air-trends>, last access: 15 Jan 2017, 2009.

785 Garzón, J. P., Huertas, J. I., Magaña, M., Huertas, M. E., Cárdenas, B., Watanabe, T., Maeda, T.,
786 Wakamatsu, S., and Blanco, S.: Volatile organic compounds in the atmosphere of Mexico City, *Atmos.*
787 *Environ.*, 119, 415-429, doi:10.1016/j.atmosenv.2015.08.014, 2015.

788 Guicherit, R., and Roemer, M.: Tropospheric ozone trends, *Chemosphere*, 2, 167-183,
789 doi:10.1016/S1465-9972(00)00008-8, 2000.

790 Hernández-Paniagua, I. Y., Lowry, D., Clemitchaw, K. C., Fisher, R. E., France, J. L., Lanoisellé, M.,
791 Ramonet, M., and Nisbet, E. G.: Diurnal, seasonal, and annual trends in atmospheric CO₂ at southwest
792 London during 2000-2012: Wind sector analysis and comparison with Mace Head, Ireland, *Atmos.*
793 *Environ.*, 105, 138-147, doi: 10.1016/j.atmosenv.2015.01.02, 2015.

794 INE (Instituto Nacional de Ecología): Cuarto almanaque de datos y tendencias de la calidad del aire en
795 20 ciudades Mexicanas 2000-2009, INE-SEMARNAT, México, D.F., 405 pp., 2011.

796 INEGI (National Institute of Statistics and Geography): XIII Censo General de Población y Vivienda 2010,
797 México, available at: <http://www.censo2010.org.mx/>, last Access: 22 May 2016, 2010.

798 INEGI (National Institute of Statistics and Geography): México en Cifras, México, available at:
799 <http://www3.inegi.org.mx/sistemas/mexicocifras/default.aspx?e=19>, last access: 22 May 2016, 2015.

800 INEGI (National Institute of Statistics and Geography): Producto Interno Bruto (GDP)-Trimestral 2016,
801 available at: <http://www.inegi.org.mx/est/contenidos/proyectos/cn/pibt/>, last access: 11 Jan 2017, 2016.

802 IPCC: Climate Change 2013: The Physical Science Basis. Contribution of Working Group I to the Fifth
803 Assessment Report of the Intergovernmental Panel on Climate Change, 2013. [Stocker, T.F., D. Qin, G.-
804 K. Plattner, M. Tignor, S.K. Allen, J. Boschung, A. Nauels, Y. Xia, V. Bex and P.M. Midgley (eds.)].
805 Cambridge University Press, Cambridge, United Kingdom and New York, NY, USA, 1535 pp., 2013.

806 Jaimes, P. M., Bravo, A. H., Sosa, E. R., Cureño, G. I., Retama, H. A., Granados, G. G., and Becerra,
807 A. E.: Surface ozone concentration trends in Mexico City Metropolitan Area, in: Proceedings of the Air
808 and Waste Management Association's Annual Conference and Exhibition AWMA, San Antonio, Texas,
809 19-22 June 2012, 3, 2273-2284, 2012.

810 Jaimes-Palomera, M., Retama, A., Elias-Castro, G., Neria-Hernández, A., Rivera-Hernández, O., and
811 Velasco, E.: Non-methane hydrocarbons in the atmosphere of Mexico City: Results of the 2012 ozone-
812 season campaign, *Atmos. Environ.*, 132, 258-275, doi:10.1016/j.atmosenv.2016.02.047, 2016.

813 Jenkin, M. E., and Clemitshaw, K. C.: Ozone and other secondary photochemical pollutants: chemical
814 processes governing their formation in the planetary boundary layer, *Atmos. Environ.*, 34(16), 2499-
815 2527, doi:10.1016/S1352-2310(99)00478-1, 2000.

816 Kanda, I., Basaldud, R., Magaña, M., Retama, A., Kubo, R., and Wakamatsu, S.: Comparison of Ozone
817 Production Regimes between Two Mexican Cities: Guadalajara and Mexico City, *Atmosphere*, 7, 91,
818 doi:10.3390/atmos7070091, 2016.

819 Lee, Y. C., Shindell, D. T., Faluvegi, G., Wenig, M., Lam, Y. F., Ning, Z., Hao, S., and Lai, C. S.: Increase
820 of ozone concentrations, its temperature sensitivity and the precursor factor in South China, *Tellus B.*
821 *Chem. Phys. Meteorol.*, 66, doi:10.3402/tellusb.v66.23455, 2014.

822 Lefohn, A. S., Shadwick, D., and Oltmans, S. J.: Characterizing changes in surface ozone levels in
823 metropolitan and rural areas in the United States for 1980-2008 and 1994-2008, *Atmos. Environ.*, 44,
824 5199-5210, doi: 10.1016/j.atmosenv.2010.08.049, 2010.

825 Lei, W., de Foy, B., Zavala, M., Volkamer, R., and Molina, L. T.: Characterizing ozone production in the
826 Mexico City Metropolitan Area: a case study using a chemical transport model, *Atmos. Chem. Phys.*, 7,
827 1347-1366, doi:10.5194/acp-7-1347-2007, 2007.

828 Lelieveld, J., Evans, J. S., Fnais, M., Giannadaki, D., and Pozzer, A.: The contribution of outdoor air
829 pollution sources to premature mortality on a global scale, *Nature Letts.*, 15371,
830 doi:10.1038/nature15371, 2015.

831 Menchaca-Torre, H. L., Mercado-Hernández, R., and Mendoza-Domínguez, A.: Diurnal and seasonal
832 variation of volatile organic compounds in the atmosphere of Monterrey, Mexico, *Atmos. Poll. Res.*, 6,
833 1073-1081, doi:10.1016/j.apr.2015.06.004, 2015.

834 Molina, M. J., and Molina, L. T.: Megacities and atmospheric pollution, *J. Air Waste Manage.*, 54, 644-
835 680, doi:10.1080/10473289.2004.10470936, 2004.

836 Monks, P. S.: A review of the observations and origins of the spring ozone maximum, *Atmos. Environ.*,
837 34, 3545-3561, doi:10.1016/S1352-2310(00)00129-1, 2000.

838 Monks, P. S., Archibald, A. T., Colette, A., Cooper, O., Coyle, M., Derwent, R., Fowler, D., Granier, C.,
839 Law, K. S., Mills, G. E., Stevenson, D. S., Tarasova, O., Thouret, V., von Schneidemesser, E.,
840 Sommariva, R., Wild, O., and Williams, M. L.: Tropospheric ozone and its precursors from the urban to
841 the global scale from air quality to short-lived climate forcer, *Atmos. Chem. Phys.*, 15, 8889-8973,
842 doi:10.5194/acp-15-8889-2015, 2015.

843 Parrish, D. D., Millet, D. B., and Goldstein, A. H.: Increasing ozone in marine boundary layer inflow at
844 the west coasts of North America and Europe, *Atmos. Chem. Phys.*, 9, 1303-1323, doi:10.5194/acp-9-
845 1303-2009, 2009.

846 Parrish, D. D., Singh, H. B., Molina, L., and Madronich, S.: Air quality progress in North American
847 megacities: A review, *Atmos. Environ.*, 45, 7015-7025, doi:10.1016/j.atmosenv.2011.09.039, 2011.

848 PICCA (Programa integral contra la contaminación atmosférica de la zona metropolitana de la Ciudad
849 de México), Mexico City Local Government, available at: http://centro.paot.org.mx/documentos/variros/prog_inte_atmosferica.pdf, last Access: 28 April 2017, 1990

851 ProAire-MMA (Programa de Gestión para Mejorar la Calidad del Aire del Área Metropolitana de
852 Monterrey 2008-2012), SEMARNAT, Gobierno del estado de Nuevo León, available at:
853 <http://www.semarnat.gob.mx/archivosanteriores/temas/gestionambiental/calidaddelaire/>
854 Documents/Calidad%20del%20aire/Proaires/ProAires_Vigentes/6_ProAire%20AMM%202008-
855 2012.pdf, last access: 22 May 2016, 2008.

856 ProAire-MCMA (Programa para Mejorar la Calidad del Aire de la Zona Metropolitana del Valle de México
857 2002-2010), Mexico City Local Government-State of Mexico Government, available at:
858 http://www.gob.mx/cms/uploads/attachment/file/69312/11_ProAire_ZMVM_2002-2010.pdf, last access:
859 28 April, 2017, 2001.

860 ProAire-MCMA (Programa para Mejorar la Calidad del Aire de la Zona Metropolitana del Valle de México
861 2002-2010), Mexico City Local Government-State of Mexico Government, available at:
862 <http://www.aire.cdmx.gob.mx/descargas/publicaciones/flippingbook/proaire2011-2020/#p=1>, last
863 access: 28 April 2017, 2011

864 Pugliese, S. C., Murphy, J. G., Geddes, J. A., and Wang, J. M.: The impacts of precursor reduction and
865 meteorology on ground-level ozone in the Greater Toronto Area, *Atmos. Chem. Phys.*, 14, 8197-8207,
866 doi:10.5194/acp-14-8197-2014, 2014.

867 Pusede, S. E., and Cohen, R. C. On the observed response of ozone to NO_x and VOC reactivity
868 reductions in San Joaquin Valley California 1995–present, *Atmos. Chem. Phys.*, 12, 8323-8339,
869 doi:10.5194/acp-12-8323-2012, 2012.

870 Pusede, S. E., Steiner, A. L., and Cohen, R.C.: Temperature and recent trends in the chemistry of
871 continental surface ozone, *Chem. Rev.*, 115, 3898-3918, doi: 10.1021/cr5006815, 2015.

872 R Core Team: R: a Language and Environment for Statistical Computing, R Foundation for Statistical
873 Computing, Vienna, Austria, ISBN 3-900051-07-0, 2013, available at: www.R-project.org, last access:
874 23 May 2016, 2013.

875 Radian (International): Mexico Emissions Inventory Program Manuals (Vol. II-VI), available at:
876 https://www3.epa.gov/ttnccatc1/cica/other3_s.html, last access: 15 Jan 2017, 2000.

877 Reinsel, G. C.: Elements of Multivariate Time Series Analysis. Springer-Verlag, New York, USA, 2nd
878 Edition, 1997.

879 Revell, L. E., Tummon, F., Stenke, A., Sukhodolov, T., Coulon, A., Rozanov, E., Garny, H., Grewe, V.
880 and Peter, T.: Drivers of the tropospheric ozone budget throughout the 21st century under the medium-
881 high climate scenario RCP 6.0, *Atmos. Chem. Phys.*, 15, 5887-5902, doi:10.5194/acp-15-5887-2015,
882 2015.

883 Rodríguez, S., Huerta, G., and Reyes, H.: A study of trends for Mexico City ozone extremes: 2001-2014,
884 *Atmosfera*, 29, 107-120, doi:10.20937/ATM.2016.29.02.01, 2016.

885 Russell, A. R., Valin, L. C., and Cohen, R. C.: Trends in OMI NO₂ observations over the United States:
886 effects of emission control technology and the economic recession, *Atmos. Chem. Phys.*, 12, 12197-
887 12209, doi:10.5194/acp-12-12197-2012, 2012.

888 Salmi, T., Määttä, A., Anttila, P., Ruoho-Airola, T. and Amnell, T.: Detecting trends of annual values of
889 atmospheric pollutants by the Mann-Kendall test and Sen's slope estimates – the Excel template
890 application MAKESENS, Publications on Air Quality Report code FMI-AQ-31, Helsinki, Finland, 31, 1-
891 35, 2002.

892 Sather, M.E. and Cavender, K.: Trends analyses of 30 years of ambient 8 hour ozone and precursor
893 monitoring data in the South Central US: progress and challenges, *Environ. Sci. Proc. Imp.*, 18, 819-
894 831. 2016.

895 Schultz, M., and Rast, S.: REanalysis of the TROpospheric chemical composition over the past 40 years,
896 Emission Data Sets and Methodologies for Estimating Emissions, Work Package 1, Deliverable D1-6,

897 available at: http://retro-archive.iek.fz-juelich.de/data/documents/reports/D1-6_final.pdf, last access: 14
898 Jul 2016, 2007.

899 SDS (Secretaria de Desarrollo Sustentable), Inventario de emisiones del Área Metropolitana de
900 Monterrey 2013, personal communication, Monterrey, N.L. México, 4 Sep 2015.

901 SDS (Secretaria de Desarrollo Sustentable): Sistema Integral de Monitoreo Ambiental, available at:
902 <http://aire.nl.gob.mx/>, last access: 21 May 2016, 2016.

903 SEDEMA (Secretaria del Medio Ambiente): INVENTARIO de Emisiones a la Atmosfera en la ZMVM
904 1996, available at: <http://www.sedema.df.gob.mx/flippingbook/inventario-emisiones-1996/#p=1>, last
905 access: 20 May 2016, 1999.

906 SEDEMA (Secretaria del Medio Ambiente): Inventario de Emisiones Zona Metropolitana del Valle de
907 Mexico 1998, available at: <http://www.sedema.df.gob.mx/flippingbook/inventario-emisiones->
908 zmvm1998/#p=75, last access: 20 May 2016, 2001.

909 SEDEMA (Secretaria del Medio Ambiente): Inventario de emisiones a la Atmosfera Zona Metropolitana
910 del Valle de Mexico 2000, available at: <http://www.sedema.df.gob.mx/> flippingbook/inventario-
911 emisiones-zmvm2000/, last access: 20 May 2016, 2003.

912 SEDEMA (Secretaria del Medio Ambiente): Inventario de emisiones de la Zona Metropolitana del Valle
913 de Mexico 2002, available at: <http://www.sedema.df.gob.mx/flippingbook/inventario-emisiones-zmvm->
914 criterio2004/#p=1, last access: 20 May 2016, 2004.

915 SEDEMA (Secretaria del Medio Ambiente): Inventario de Emisiones Zona Metropolitana del Valle de
916 Mexico 2004, available at: <http://www.sedema.df.gob.mx/flippingbook/inventario-emisiones-zmvm->
917 criterio2004/#p=1, last access: 20 May 2016, 2006.

918 SEDEMA (Secretaria del Medio Ambiente): Inventario de Emisiones de Contaminantes Criterio 2006,
919 available at: <http://www.sedema.df.gob.mx/flippingbook/inventario-emisiones-zmvm-criterio2006/#p=1>,
920 last access: 20 May 2016, 2008.

921 SEDEMA (Secretaria del Medio Ambiente): Inventario de emisiones de contaminantes criterio de la
922 ZMVM 2008, available at: <http://www.sedema.df.gob.mx/flippingbook/inventario-emisiones-zmvm->
923 criterio2008/#p=1, last access: 20 May 2016, 2010.

924 SEDEMA (Secretaria del Medio Ambiente): Inventario de emisiones de la Zona Metroplitana del Valle
925 de Mexico contaminantes criterio 2010, available at:
926 <http://www.sedema.df.gob.mx/flippingbook/inventario-emisiones-zmvm-criterio-2010/#p=6>, last
927 access: 20 May 2016, 2012.

928 SEDEMA (Secretaria del Medio Ambiente): Inventario de Emisiones Contaminantes y de efecto
929 invernadero, available at: <http://www.sedema.df.gob.mx/flippingbook/inventario-emisioneszmvm2012/>,
930 last access: 20 May 2016, 2014.

931 SEDEMA (Secretaria del Medio Ambiente de la Ciudad de Mexico): Sistema de Monitoreo Atmosférico,
932 available at: <http://www.aire.df.gob.mx/default.php>, last access: 21 May 2016, 2016a.

933 SEDEMA (Secretaria del Medio Ambiente de la Ciudad de Mexico): Inventario de Emisiones de la CDMX
934 2014 Contaminantes Criterio Tóxicos y de Efecto Invernadero, available at:
935 <http://www.aire.cdmx.gob.mx/descargas/publicaciones/flippingbook/inventario-emisiones-cdmx2014-2/>,
936 last Access: 10 Jan 2017, 2016b.

937 SEMARNAT (Secretaria del Medio Ambiente y Recursos Naturales): NOM-041 (NORMA OFICIAL
938 MEXICANA, QUE ESTABLECE LOS LIMITES MAXIMOS PERMISIBLES DE EMISION DE GASES
939 CONTAMINANTES PROVENIENTES DEL ESCAPE DE LOS VEHICULOS AUTOMOTORES EN
940 CIRCULACION QUE USAN GASOLINA COMO COMBUSTIBLE), Diario Oficial de la Federación, 1993.

941 SEMARNAT (Secretaria del Medio Ambiente y Recursos Naturales): NOM-042 (NORMA OFICIAL
942 MEXICANA QUE ESTABLECE LOS LIMITES MAXIMOS PERMISIBLES DE EMISION DE
943 HIDROCARBUROS TOTALES O NO METANO, MONOXIDO DE CARBONO, OXIDOS DE
944 NITROGENO Y PARTICULAS PROVENIENTES DEL ESCAPE DE LOS VEHICULOS
945 AUTOMOTORES NUEVOS CUYO PESO BRUTO VEHICULAR NO EXCEDA LOS 3,857
946 KILOGRAMOS, QUE USAN GASOLINA, GAS LICUADO DE PETROLEO, GAS NATURAL Y DIESEL,
947 ASI COMO DE LAS EMISIONES DE HIDROCARBUROS EVAPORATIVOS PROVENIENTES DEL
948 SISTEMA DE COMBUSTIBLE DE DICHOS VEHICULOS), Diario Oficial de la Federación, 1993.

949 SEMARNAT (Secretaria del Medio Ambiente y Recursos Naturales): Inventario Nacional de Emisiones
950 1999, México, D.F., available at: <http://www.inecc.gob.mx/dica/548-calaire-inem-1999>, last access: 20
951 May 2016, 2006.

952 SEMARNAT (Secretaria del Medio Ambiente y Recursos Naturales): Inventario Nacional de Emisiones
953 2005, México, D.F., available at: <http://sinea.semarnat.gob.mx/sinae.php?process=UkVQT1JURUFET1I=&categ=1>, last access: 22 May 2016, 2011.

955 SEMARNAT (Secretaria del Medio Ambiente y Recursos Naturales): Inventario Nacional de Emisiones
956 2008, México, D.F., available at: <http://sinea.semarnat.gob.mx/sinae.php?process=UkVQT1JURUFET1I=&categ=14>, last access: 22 May 2016, 2014.

958 SEMARNAT (Secretaria del Medio Ambiente y Recursos Naturales): Informe Nacional de calidad del
959 aire 2014, México, D.F., available at: http://inecc.gob.mx/descargas/calaire/2015_Informe_nacional_calidad_aire_2014_Final.pdf, last access: 15 Dec 2016, 2015.

961 SENER (Secretaria de Energia): Estadísticas Energéticas Nacionales, México, available at:
962 <http://sie.energia.gob.mx/bdiController.do?action=temas>, last access: 4 November 2015, 2015.

963 Sicard, P., Serra, R., and Rossello, P.: Spatiotemporal trends in ground-level ozone concentrations and
964 metrics in France over the time period 1999-2012, Environ. Res., 149, 122-144,
965 doi:10.1016/j.envres.2016.05.014, 2016

966 Sierra, A., Vanoye, A. Y., and Mendoza, A.: Ozone sensitivity to its precursor emissions in northeastern
967 Mexico for a summer air pollution episode, J. Air Waste Manage., 63, 1221-1233,
968 doi:10.1080/10962247.2013.813875, 2013.

969 Simon, H., Reff, A., Wells, B., Xing, J., and Frank, N.: Ozone trends across the United States over a
970 period of decreasing NO_x and VOC emissions, Environ. Sci. Tech., 49, 186-195. doi:10.1021/es504514z,
971 2015.

972 SMN (Servicio Meteorológico Nacional), available at: <http://smn.cna.gob.mx/es/>, last access: 21 May
973 2016.

974 Staehelin, J., and Schmid, W.: Trend analysis of tropospheric ozone concentrations utilizing the 20-year
975 data set of ozone balloon soundings over Payerne (Switzerland), Atmos. Environ., 25, 1739-1749,
976 doi:10.1016/0960-1686(91)90258-9, 1991.

977 Stein, A. F., Draxler, R. R., Rolph, G. D., Stunder, B. J. B., Cohen, M. D., and Ngan, F.: NOAA'S HYSPLIT
978 atmospheric transport and dispersion modelling system. Am. Meteorol. Soc., 96, 2059-2077,
979 doi:10.1175/BAMS-D-14-00110.1, 2015.

980 Stephens, S., Madronich, S., Wu, F., Olson, J. B., Ramos, R., Retama, A., and Muñoz, R.: Weekly
981 patterns of México City's surface concentrations of CO, NO_x, PM₁₀ and O₃ during 1986-2007, Atmos.
982 Chem. Phys., 8, 5313-5325, doi:10.5194/acp-8-5313-2008, 2008.

983 Stevenson, D. S., Dentener, F. J., Schultz, M. G., Ellingsen, K., van Noije, T. P. C., Wild, O., Zeng, G.,
984 Amann, M., Atherton, C. S., Belli, N., Bergmann, D. J., Bey, I., Butler, T., Cofala, J., Collins, W. J.,
985 Derwent, R. G., Doherty, R. M., Drevet, J., Eskes, H. J., Fiore, A. M., Gauss, M., Hauglustaine, D. A.,
986 Horowitz, L. W., Isaksen, I. S. A., Krol, M. C., Lamarque, J.-., Lawrence, M. G., Montanaro, V., Müller,
987 J.-., Pitari, G., Prather, M. J., Pyle, J. A., Rast, S., Rodriguez, J. M., Sanderson, M. G., Savage, N. H.,

988 Shindell, D. T., Strahan, S. E., Sudo, K., and Szopa, S.: Multimodel ensemble simulations of present-
989 day and near-future tropospheric ozone. *J. Geophys. Res.*, D08301, doi: 10.1029/2005JD006338, 2006.

990 Strode, S. A., Rodriguez, J. M., Logan, J. A., Cooper, O. R., Witte, J. C., Lamsal, L. N., Damon, M., Van
991 Aartsen, B., Steenrod, S. D., and Strahan, S. E.: Trends and variability in surface ozone over the United
992 States. *J. Geophys. Res.*, 120, 9020-9042, doi:10.1002/2014JD022784, 2015.

993 Tiwari, A. K., Suresh, K. G., Arouri, M., and Teulon, F.: Causality between consumer price and producer
994 price: Evidence from Mexico, *Econ. Model.*, 36, 432-440, doi:10.1016/j.econmod.2013.09.050, 2014.

995 Torres-Jardon, R., García-Reynoso, J. A., Jazcilevich, A., Ruiz-Suárez, L. G., and Keener, T. C.:
996 Assessment of the ozone-nitrogen oxide-volatile organic compound sensitivity of Mexico City through an
997 indicator-based approach: measurements and numerical simulations comparison, *J. Air Waste Manag.
998 Assoc.*, 59, 1155-1172, doi:10.3155/1047-3289.59.10.1155, 2009.

999 VanCuren, R.: Transport aloft drives peak ozone in the Mojave Desert, *Atmos. Environ.*, 109, 331-341,
1000 doi: 10.1016/j.atmosenv.2014.09.057, 2015.

1001 Vingarzan, R.: A review of surface ozone background levels and trends, *Atmos. Environ.*, 38, 3431-3442,
1002 doi:10.1016/j.atmosenv.2004.03.030, 2004.

1003 Velasco, E., Lamb, B., Westberg, H., Allwine, E., Sosa, G., Arriaga-Colina, J. L., Jobson, B. T.,
1004 Alexander, M. L., Prazeller, P., Knighton, W. B., Rogers, T. M., Grutter, M., Herndon, S. C., Kolb, C. E.,
1005 Zavala, M., de Foy, B., Volkamer, R., Molina, L. T., and Molina, M. J.: Distribution, magnitudes,
1006 reactivities, ratios and diurnal patterns of volatile organic compounds in the Valley of Mexico during the
1007 MCMA 2002 & 2003 field campaigns, *Atmos. Chem. Phys.*, 7, 329-353, doi:10.5194/acp-7-329-2007,
1008 2007.

1009 Wang, Y., Konopka, P., Liu, Y., Chen, H., Müller, R., Plöger, F., Riese, M., Cai, Z., and Lü, D.:
1010 Tropospheric ozone trend over Beijing from 2002-2010: Ozonesonde measurements and modeling
1011 analysis, *Atmos. Chem. Phys.*, 12, 8389-8399, doi:10.5194/acp-12-8389-2012, 2012.

1012 Wilson, R. C., Fleming, Z. L., Monks, P. S., Clain, G., Henne, S., Konovalov, I. B., Szopa, S., and Menut,
1013 L.: Have primary emission reduction measures reduced ozone across Europe? An analysis of European
1014 rural background ozone trends 1996-2005, *Atmos. Chem. Phys.*, 12, 437-454, doi:10.5194/acp-12-437-
1015 2012, 2012.

1016 Wolff, G. T., Kahlbaum, D. F., and Heuss, J. M.: The vanishing ozone weekday/weekend effect, *J. Air
1017 Waste Manage.*, 63, 292-299, doi:10.1080/10962247.2012.749312, 2013.

1018 World Health Organization: Ambient (outdoor) air quality and health, 2014 update,
1019 <http://www.who.int/mediacentre/factsheets/fs313/en/>, last access: 21 May 2016.

1020 Xing, J., Pleim, J., Mathur, R., Pouliot, G., Hogrefe, C., Gan, C.-M., and Wei, C.: Historical gaseous and
1021 primary aerosol emissions in the United States from 1990 to 2010, *Atmos. Chem. Phys.*, 13, 7531-7549,
1022 doi:10.5194/acp-13-7531-2013, 2013.

1023 Xu, X., Lin, W., Wang, T., Yan, P., Tang, J., Meng, Z., and Wang, Y.: Long-term trend of surface ozone
1024 at a regional background station in eastern China 1991-2006: Enhanced variability, *Atmos. Chem. Phys.*,
1025 8, 2595-2607, doi:10.5194/acp-8-2595-2008, 2008.

1026 Zellweger, C., Hüglin, C., Klausen, J., Steinbacher, M., Vollmer, M., and Buchmann, B.: Inter-comparison
1027 of four different carbon monoxide measurement techniques and evaluation of the long-term carbon
1028 monoxide time series of Jungfraujoch, *Atmos. Chem. Phys.*, 9, 3491-3503, doi:10.5194/acp-9-3491-
1029 2009, 2009.

1030 Zheng, J., Swall, J. L., Cox, W. M., and Davis, J. M. Interannual variation in meteorologically adjusted
1031 ozone levels in the eastern United States: A comparison of two approaches, *Atmos. Environ.*, 41, 705-
1032 716, doi:10.1016/j.atmosenv.2006.09.010, 2007.

Table 1. Air quality limit values stated in Mexican legislation.

Pollutant	Mexican Official Standard	Limit value*
O ₃ (ppb)	NOM-020-SSA1-1993	110 (1-h), 80 (8-h) ^{a,b}
	NOM-020-SSA1-2014	95 (1-h) , 70 (8-h) ^{a,b}
PM ₁₀ (µg m ⁻³)	NOM-025-SSA1-1993	75 (24-h), 40 (1-yr)
	NOM-025-SSA1-2014	50 (24h), 35 (1-yr)
PM _{2.5} (µg m ⁻³)	NOM-025-SSA1-1993	45 (24-h), 12 (1-yr)
	NOM-025-SSA1-2014	30 (24-h), 10 (1-yr)
CO (ppm)	NOM-02-SSA1-1993	11 (8-h) ^b
NO ₂ (ppm)	NOM-023-SSA1 -1993	0.21 (1-h)

1034 *Average period.

1035 ^aNot to be exceeded more than 4 times in a calendar year.1036 ^bRunning average.

1037

1038

Table 2. Site description, location and instrumentation used during 1993 to 2014 within the MMA.

Site	Code	Location	Elevation (m a.s.l.)	Site description
Guadalupe	GPE	25° 40.110' N, 100° 14.907' W	492	Urban background site in the La Pastora park, surrounded by a highly populated area, 450 m from Pablo Rivas Rd.
San Nicolas	SNN	25° 44.727' N, 100° 15.301' W	476	Urban site surrounded by a large number of industries and residential areas, 450 m from Juan Diego Diaz de Beriagna Rd.
Obispado	OBI	25° 40.561' N, 100° 20.314' W	560	Urban site near the city centre of MMA, 250 m from Jose Eleuterio González Rd. and 250 m from Antonio L. Rodríguez Rd.
San Bernabe	SNB	25° 45.415' N, 100° 21.949' W	571	Urban site in a residential area downwind of an industrial area with high traffic volume, 140 m from Aztlan Rd.
Santa Catarina	STA	25° 40.542' N, 100° 27.901' W	679	Urban site downwind of industrial sources, 200 m from Manuel Ordoñez Rd.

1040

1041

1042

1043

1044

1045

1046

1047

1048

1049

1050

1051

1052

1053

1054

1055

1056

1057

1058 **Table 3.** Results for O_3 and O_x long-term trends expressed in ppb yr^{-1} for 1993-2014 at the 5 sites within
 1059 the MMA by season.

Site	Period	Ozone (O_3)			Odd oxygen ($O_x = O_3 + NO_2$)		
		ppb yr^{-1}	% yr^{-1}	Significance	ppb yr^{-1}	% yr^{-1}	Significance
GPE	Annual	0.21	0.78	*	0.31	0.80	**
	Spring	0.24	0.73	*	0.32	0.69	*
	Summer	0.30	1.16	*	0.38	1.18	*
	Autumn	0.14	0.53		0.25	0.62	
	Winter	0.12	0.53		0.14	0.33	*
SNN	Annual	0.33	1.40	***	0.45	1.25	*
	Spring	0.39	1.38	*	0.49	1.22	*
	Summer	0.47	2.24	*	0.58	1.87	***
	Autumn	0.41	1.96	*	0.65	1.94	*
	Winter	0.14	0.68		0.23	0.58	+
OBI	Annual	0.30	1.29	*	-0.17	-0.35	
	Spring	0.43	1.56	*	0.02	0.03	*
	Summer	0.26	0.98	*	-0.04	-0.09	
	Autumn	0.29	1.33	+	-0.66	-1.15	
	Winter	0.25	1.46		-0.28	-0.53	
SNB	Annual	0.19	0.65	+	0.61	1.66	**
	Spring	0.37	1.07	+	0.67	1.65	+
	Summer	0.31	1.06	***	0.66	2.17	***
	Autumn	0.19	0.64		0.60	1.61	+
	Winter	0.02	0.07		0.47	1.12	+
STA	Annual	0.01	0.01		-0.15	-0.28	
	Spring	-0.04	-0.11		-0.01	-0.02	
	Summer	0.09	0.28		0.13	0.27	
	Autumn	0.00	0.00		-0.22	-0.41	
	Winter	-0.09	-0.43		-0.63	-1.15	*

1060 ⁺Level of significance $p < 0.1$.

1061 ^{*}Level of significance $p < 0.05$.

1062 ^{**}Level of significance $p < 0.001$.

1063 ^{***}Level of significance $p < 0.001$.

1064

1065

1066

1067

1068

1069

1070

1071 **Table 4.** Results for O₃ and O_x long-term trends by season expressed in ppb yr⁻¹ during 1993-2014 for
 1072 the MCMA and MMA, and during 1996-2014 for the GMA.

Urban area	Period	Ozone (O ₃)			Odd oxygen (O ₃ + NO ₂)		
		ppb yr ⁻¹	% yr ⁻¹	Significance	ppb yr ⁻¹	% yr ⁻¹	Significance
MCMA	Annual	-1.15	-2.04	***	-1.87	-1.94	***
	Spring	-0.97	-1.53	***	-1.77	-1.71	***
	Summer	-0.97	-1.88	***	-1.44	-1.67	***
	Autumn	-1.12	-2.20	***	-1.89	-2.15	***
	Winter	-1.62	-2.64	***	-2.47	-2.27	***
GMA	Annual	-0.29	-0.81		-1.46	-1.85	+
	Spring	-0.26	-0.57		-1.89	-2.07	*
	Summer	-0.10	-0.32		-1.43	-1.89	*
	Autumn	-0.09	0.33		-1.40	-1.97	*
	Winter	-0.34	-1.01		-1.74	-2.08	***
MMA	Annual	0.22	0.84	**	0.13	0.30	
	Spring	0.32	1.04	**	0.29	0.63	
	Summer	0.27	0.99	***	0.28	0.72	***
	Autumn	0.25	1.03		0.13	0.31	
	Winter	0.10	0.45		0.01	-0.01	

1073 ⁺Level of significance $p < 0.1$.

1074 ^{*}Level of significance $p < 0.05$.

1075 ^{**}Level of significance $p < 0.001$.

1076 ^{***}Level of significance $p < 0.001$.

1077

1078

1079

1080

1081

1082

1083

1084

1085

1086

1087

1088

1089

1090

1091

1092 **Table 5.** Results for O₃ daily maxima long-term trends by season in ppb yr⁻¹ during 1993-2014 at the 5
 1093 sites within the MMA.

Site	Period	Ozone (O ₃)		
		ppb yr ⁻¹	% yr ⁻¹	Significance
GPE	Annual	0.45	1.02	**
	Spring	0.48	0.94	**
	Summer	0.64	1.50	*
	Autumn	0.35	0.74	
	Winter	0.26	0.63	
SNN	Annual	0.79	2.13	***
	Spring	0.87	2.01	***
	Summer	0.85	2.42	***
	Autumn	0.93	2.73	*
	Winter	0.44	1.29	
OBI	Annual	0.65	1.51	*
	Spring	0.78	1.62	**
	Summer	0.53	1.10	*
	Autumn	0.75	1.77	
	Winter	0.21	0.55	
SNB	Annual	0.40	0.80	***
	Spring	0.85	1.58	***
	Summer	0.67	1.36	***
	Autumn	0.52	1.05	*
	Winter	0.05	0.10	
STA	Annual	0.01	-0.01	
	Spring	-0.05	-0.09	
	Summer	0.22	0.35	
	Autumn	-0.07	-0.12	
	Winter	-0.35	-0.75	+

1094 ⁺Level of significance $p < 0.1$.

1095 ^{*}Level of significance $p < 0.05$.

1096 ^{**}Level of significance $p < 0.001$.

1097 ^{***}Level of significance $p < 0.001$.

1098

1099

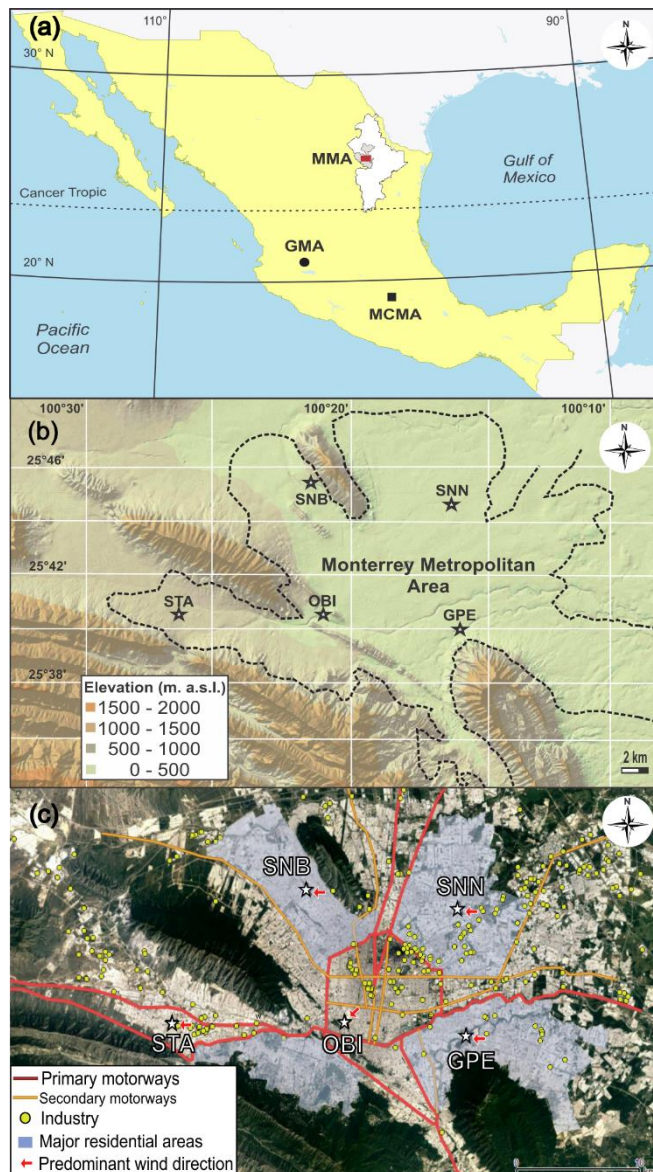
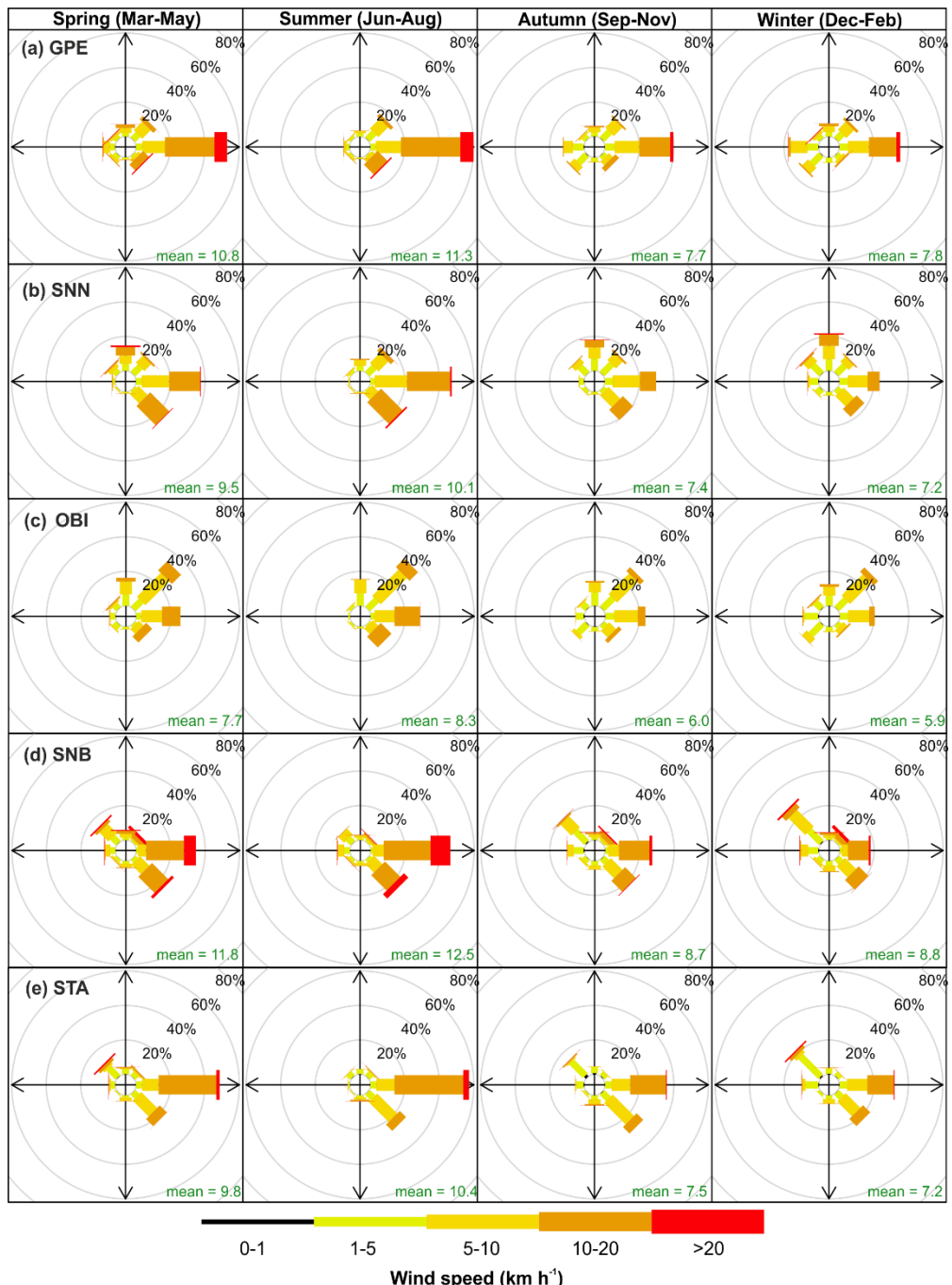
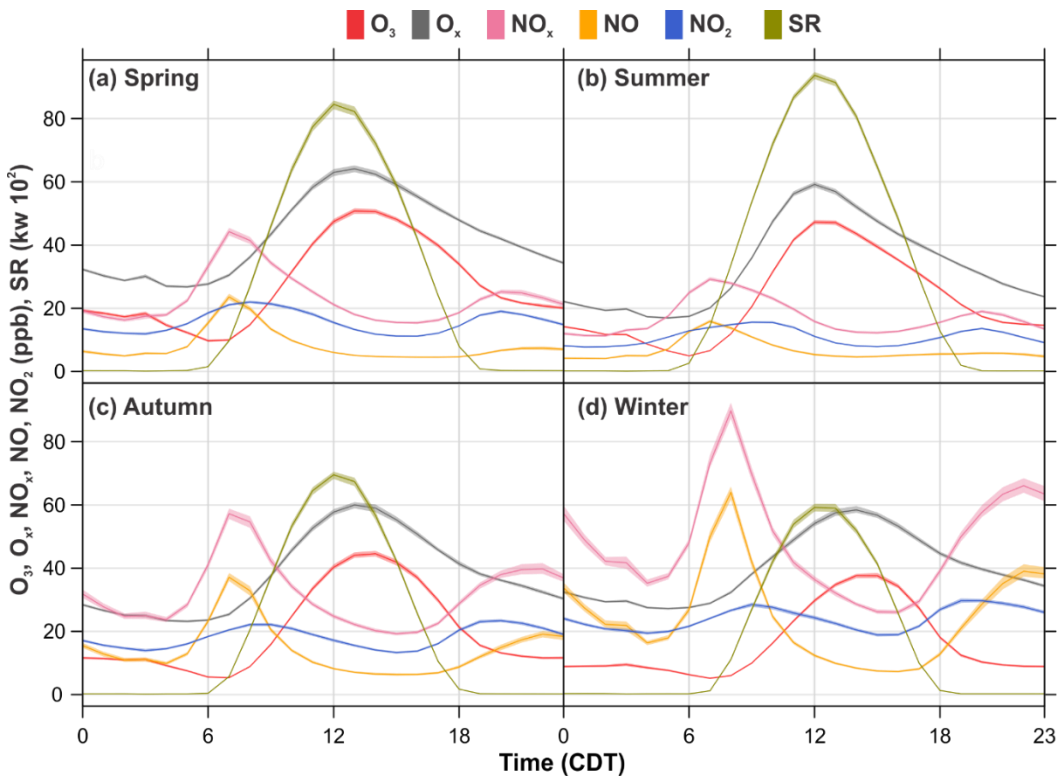


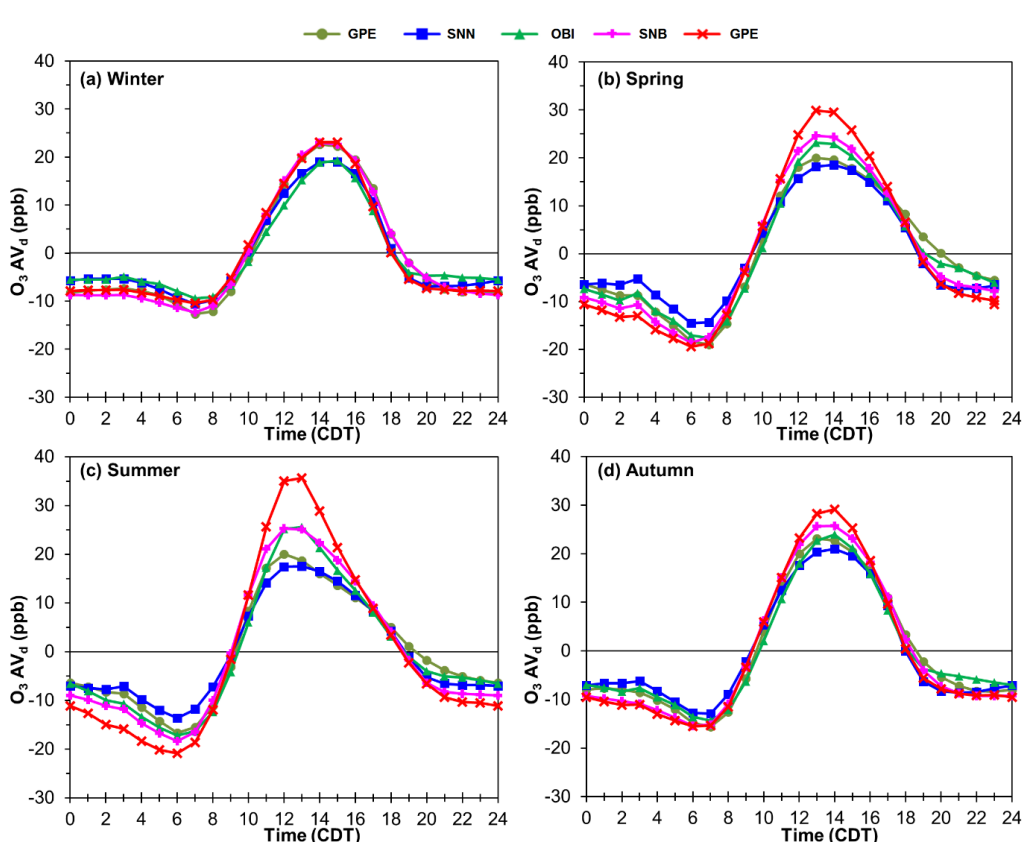
Fig. 1(a). The MMA, MCMA and GMA in the national context. **(b).** Topography of the MMA and distribution of the 5 monitoring sites over the area. **(c).** The 5 monitoring sites in relation to primary and secondary motorways, industries and major residential areas. The red arrows show the predominant wind direction at each site during 1993 to 2014.



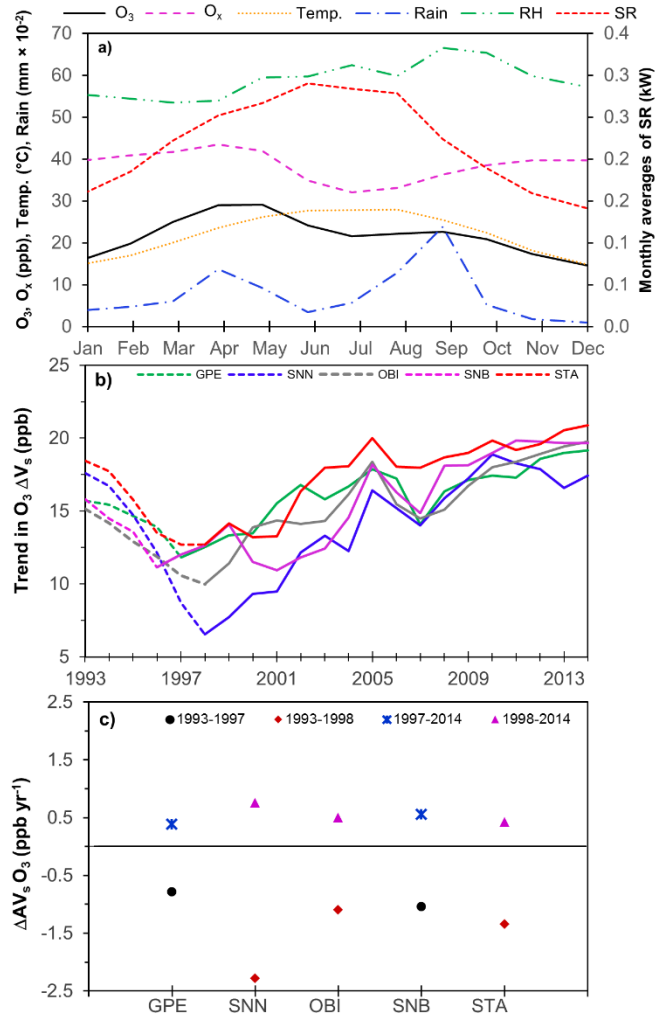
1108
1109 **Fig. 2.** Frequency of counts of measured wind direction occurrence by season and site within the MMA
1110 during 1993-2014.
1111



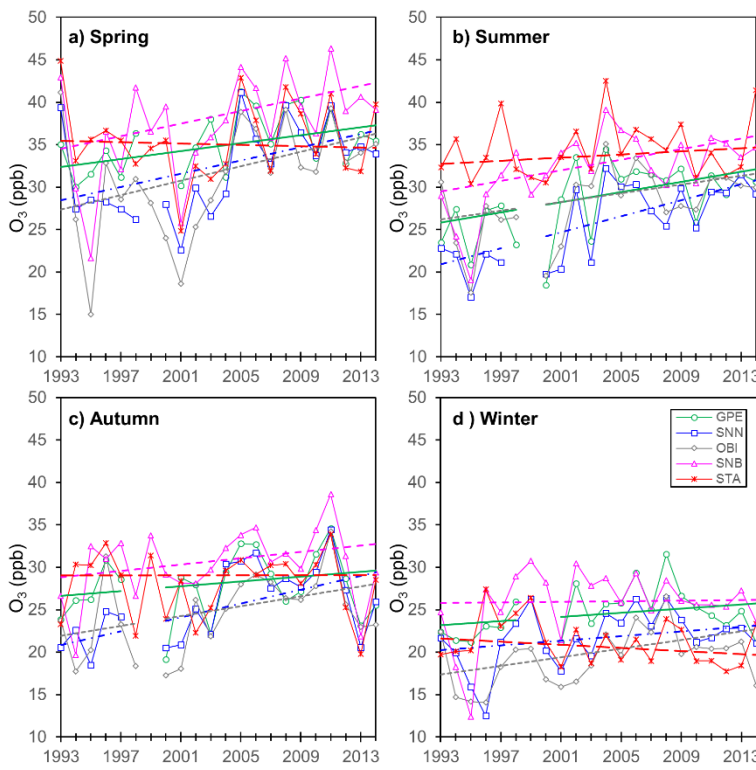
1112
 1113 **Fig. 3.** Seasonal average daily profiles for O_3 , O_x , NO_x , NO , NO_2 and SR within the MMA during 1993-
 1114 2014. The shading shows the 95 % confidence intervals of the average.
 1115



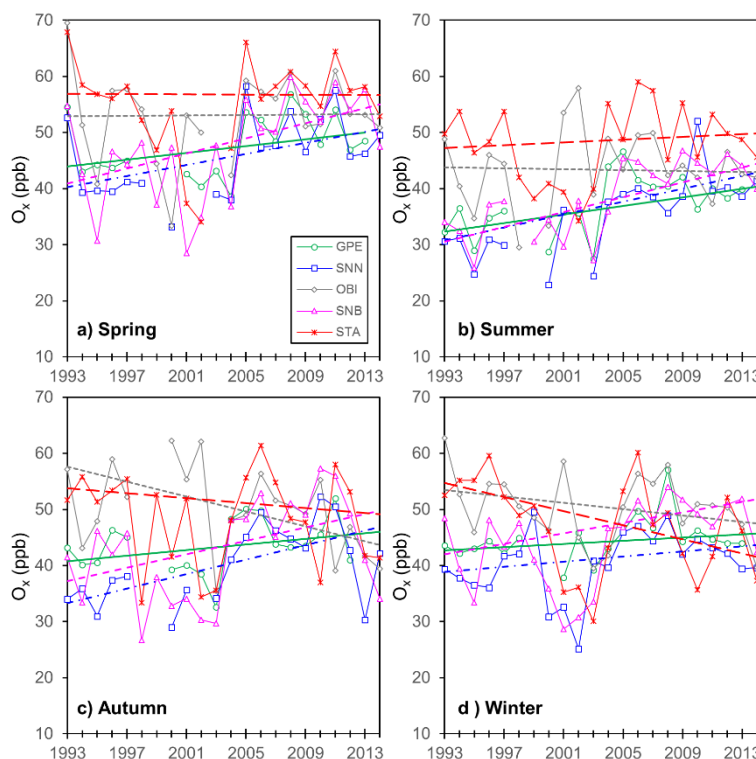
1116
 1117 **Fig. 4.** Seasonal O_3 de-trended daily profiles within the MMA during 1993-2014. De-trended O_3 daily
 1118 cycles were constructed by subtracting daily averages from hourly averages to remove the impact of
 1119 long-term trends.
 1120



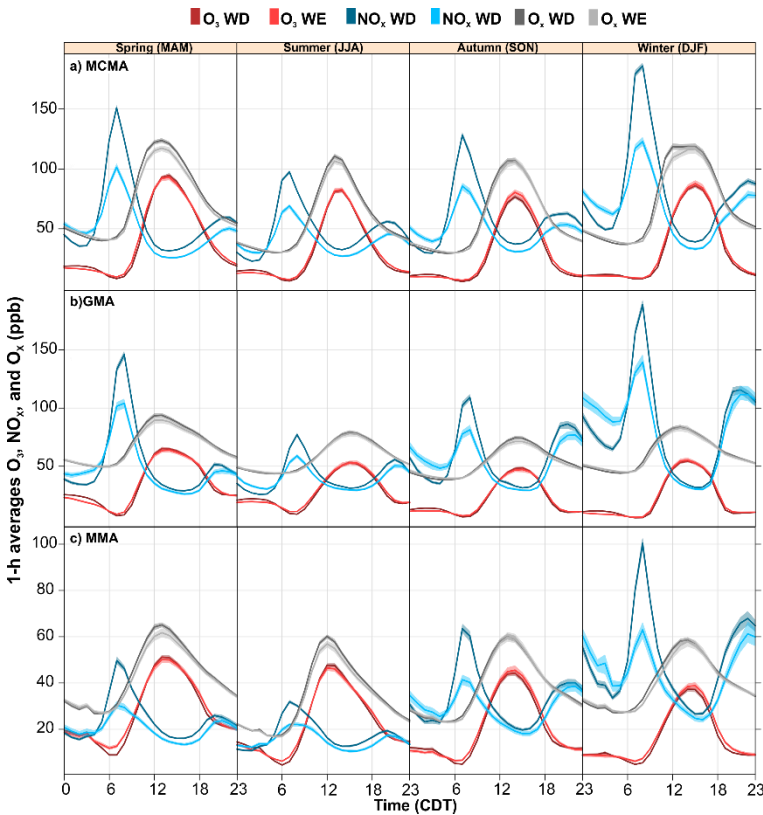
1121
1122 **Fig. 5a).** Annual cycles of O_3 , temperature, rainfall, RH and SR constructed by averaging records from
1123 1993 to 2014 for a 1-year period. **b).** Trends in AV_s of O_3 recorded at the 5 monitoring sites within the
1124 MMA from 1993 to 2014. The decline in AV_s observed is due to the economic crisis experienced in
1125 Mexico during 1994-1996, followed by persistent increases in AV_s since 1998. **c).** Annual rates of change
1126 in $O_3 AV_s$ by site, before and after the 1994-1996 economic crisis.
1127



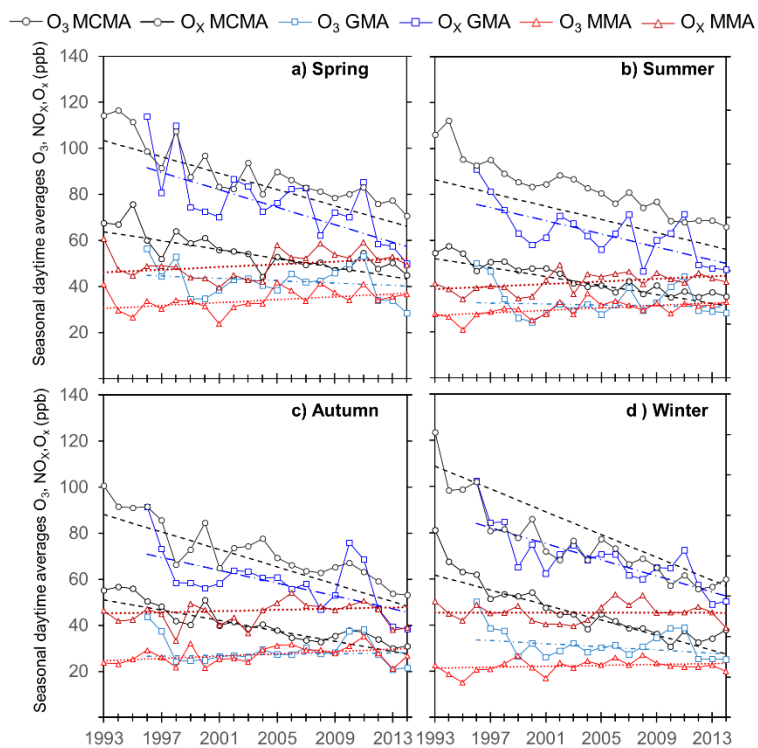
1128
 1129 **Fig. 6.** Seasonal trends of O_3 within the MMA during 1993-2014. Each data point represents the average
 1130 of the 3-month period that defines the season. The continuous lines show the Sen trend.
 1131



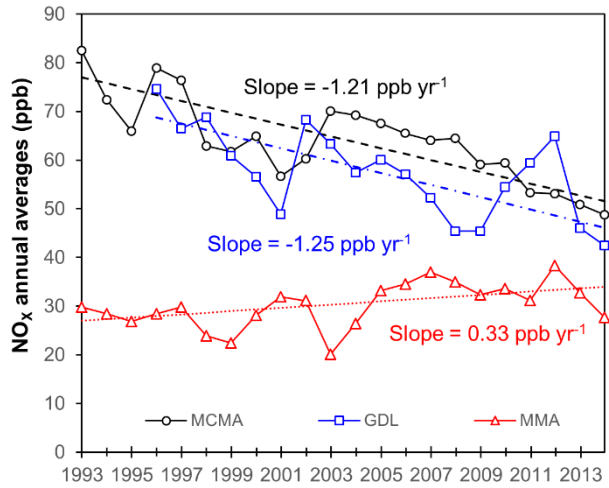
1132
 1133 **Fig. 7.** Seasonal trends of O_X within the MMA during 1993-2014. Each data point represents the average
 1134 of the 3-month period that defines the season. The continuous lines show the Sen trend.
 1135



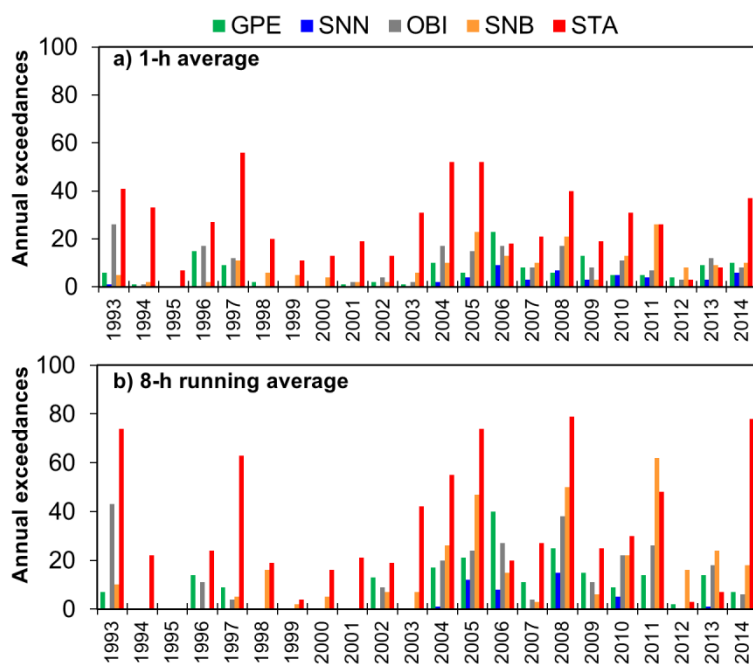
1136
1137 **Fig. 8.** Seasonal average diurnal cycles of O_3 , O_x and NO_x during 1993-2014 for the MCMA and the
1138 MMA, and between 1996-2014 for the GMA. The shading shows the 95% confidence intervals of the
1139 average, calculated through bootstrap resampling (Carslaw, 2015).
1140
1141



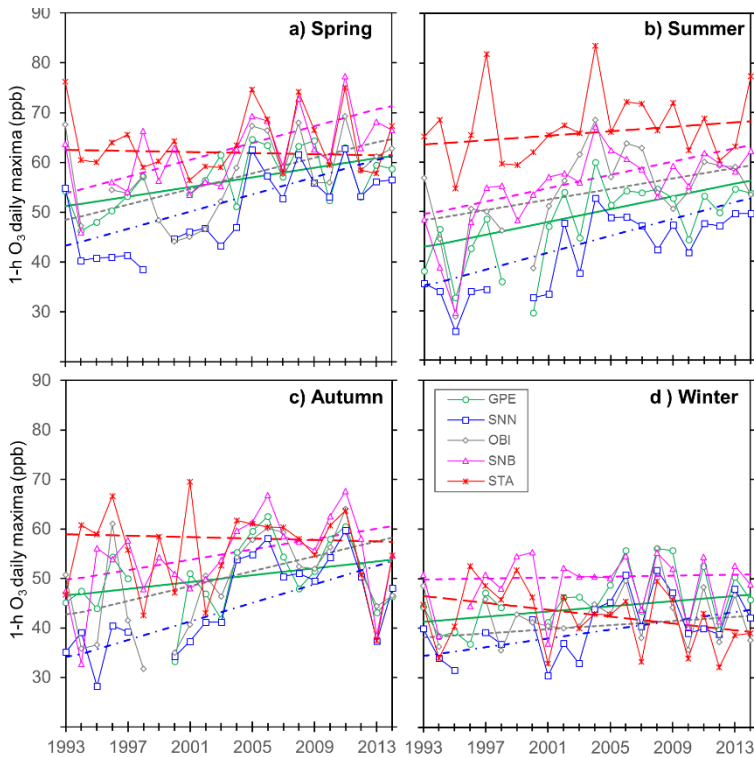
1142
1143 **Fig. 9.** Seasonal trends in O_3 and O_x for the MCMA and MMA during 1993-2014, and for the GMA during
1144 1996-2014. Each data point represents the average of the 3-month period that defines the season. The
1145 dashed lines show the Sen trend.
1146



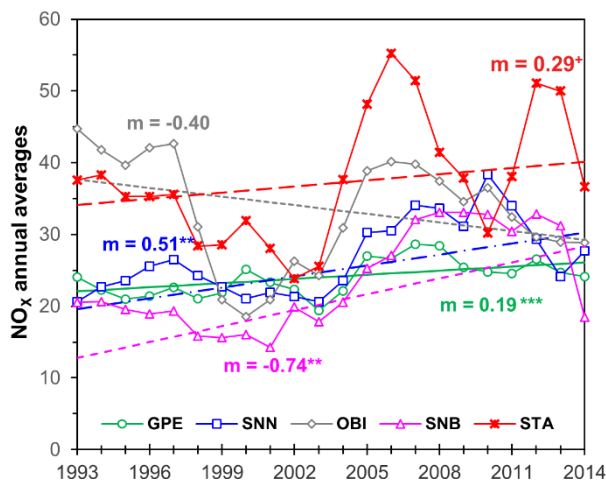
1147
1148 **Fig. 10.** Trends for NO_x at the MCMA and MMA during 1993-2014, and at the GMA during 1996-2014.
1149 The dashed lines represent the Sen slopes. All trends are statistically significant at $p < 0.05$.
1150



1151
1152 **Fig. 11.** Annual exceedances of the O₃ NOM for 1-h averages (110 ppb) and 8-h running averages (80
1153 ppb) at the 5 monitoring sites within the MMA from 1993 to 2014.
1154



1155
1156 **Fig. 12.** Seasonal trends in 1-h O₃ daily maxima at the MMA during 1993-2014. Each data point
1157 represents the average of the 3-month period that defines the season. The dashed lines show the Sen
1158 trend.
1159
1160
1161



1162
1163 **Fig. 13.** Long-term trends for NO_x at the 5 monitoring sites within the MMA during 1993-2014. The
1164 dashed lines represent the Sen slopes. Annual NO_x rates of change are described as m for slope and
1165 expressed in units of ppb yr⁻¹. Levels of confidence are represented as ⁺ = $p < 0.1$, ^{*} = $p < 0.05$, ^{**} = $p < 0.001$,
1166 ^{***} = $p < 0.001$.
1167
1168